Diimine supported group 10 hydroxo, oxo, amido, and imido complexes†

Anupam Singh,[a] U. Anandhi,[a] Maria Agostina Cinellu[b] and Paul R. Sharp*[a]

Received 11th October 2007, Accepted 29th January 2008
First published as an Advance Article on the web 4th March 2008
DOI: 10.1039/b715663d

A series of L_2 = diimine (Bian = bis(3,5-diisopropylphenylimino)acenapthene, Bu^t_2bpy = 4,4′-di-*tert*-butyl-2,2′-bipyridine) supported aqua, hydroxo, oxo, amido, imido, and mixed complexes have been prepared. Deprotonation of $[L_2Pt(\mu\text{-}OH)]_2^{2+}$ with 1,8-bis(dimethylamino)naphthalene, NaH, or KOH yields $[(L_2Pt)_2(\mu\text{-}OH)(\mu\text{-}O)]^+$ as purple (Bian) or red (Bu^t_2bpy) solids. Excess KOH gives dark blue $[(Bian)Pt(\mu\text{-}O)]_2$. MeOTf addition to $[(Bu^t_2bpy)_2Pt_2(\mu\text{-}OH)(\mu\text{-}O)]^+$ gives $[(Bu^t_2bpy)_2Pt_2(\mu\text{-}OH)(\mu\text{-}OMe)]^{2+}$ while $[(Bian)Pt(\mu\text{-}O)]_2$ yields $[(Bian)_2Pt_2(\mu\text{-}OMe)(\mu\text{-}O)]^+$. Treatment of $[(Bian)Pt(\mu\text{-}O)]_2$ with "$(Ph_3P)Au^+$" gives deep purple $[(Bian)_2Pt_2(\mu\text{-}O)(\mu\text{-}OAuPPh_3)]^+$ while $(COD)Pt(OTf)_2$ gives a low yield of $[(Bian)Pt_3(\mu\text{-}OH)_3(COD)_2](OTf)_3$. $Ni(Bu^t_2bpy)Cl_2$ and $[(Ph_3PAu)_3(\mu\text{-}O)]^+$ in a 3 : 2 ratio yield red $[Ni_3(Bu^t_2bpy)_3(\mu\text{-}O)_2]^{2+}$. $M(Bu^t_2bpy)Cl_2$ (M = Pd, Pt) and $[(Ph_3PAu)_3(\mu\text{-}O)]^+$ give $[M(Bu^t_2bpy)(\mu\text{-}OAuPPh_3)]_2^{2+}$ and $[Pd_4(Bu^t_2bpy)_4(\mu\text{-}OAuPPh_3)]^{3+}$. Addition of $ArNH_2$ to $[M(Bu^t_2bpy)(\mu\text{-}OH)]_2^{2+}$ (M = Pd, Pt) gives $[Pt_2(Bu^t_2bpy)_2(\mu\text{-}NHAr)(\mu\text{-}OH)]^{2+}$ (Ar = Ph, 4-tol, 4-$C_6H_4NO_2$) and $[M(Bu^t_2bpy)(\mu\text{-}NHAr)]_2^{2+}$ (Ar = Ph, tol). Deprotonation of $[Pt_2(Bu^t_2bpy)_2(\mu\text{-}NH\text{-}tol)(\mu\text{-}OH)]^{2+}$ with 1,8-bis(dimethylamino)naphthalene or NaH gives $[Pt_2(Bu^t_2bpy)_2(\mu\text{-}NH\text{-}tol)(\mu\text{-}O)]^+$. Deprotonation of $[Pt(Bu^t_2bpy)(\mu\text{-}NH\text{-}tol)]_2^{2+}$ with $KOBu^t$ gives deep green $[Pt(Bu^t_2bpy)(\mu\text{-}N\text{-}tol)]_2$. The triflate complexes $M(Bu^t_2bpy)(OTf)_2$ (M = Pd, Pt) are obtained from $M(Bu^t_2bpy)Cl_2$ and AgOTf. Treatment of $Pt(Bu^t_2bpy)(OTf)_2$ with water gives the aqua complex $[Pt(Bu^t_2bpy)(H_2O)_2](OTf)_2$.

Introduction

Complexes with late transition metals bonded to hydroxo, amido, oxo and imido ligands[1–5] have attracted wide attention for their conflicting soft acid–hard base interactions and their relevance in several areas including chemotherapy drugs,[6,7] enzyme modeling,[8–15] and various catalytic and stoichiometric processes.[1,16–27] Our efforts have been primarily focused on the synthesis of oxo and imido complexes of the heavier late transition metals Rh, Ir, Pd, Pt, and Au.[5] Our simplest approach to these oxo and imido complexes is deprotonation of the conjugate-acid hydroxo and amido complexes. This has required the simultaneous development of the hydroxo and amido chemistry. The majority of these hydroxo and amido complexes bear supporting phosphine ligands and our initial attempts to expand to N-donor ligand systems such as pyridine and bipyridine met with limited success due to the poor solubility of the complexes. Solubility problems were overcome with substituted cyclic and acyclic diimine ligands and we reported the synthesis and characterization of hydroxo and amido complexes of Pt(II) and Pd(II) bearing various diimine ligands.[28] However, efforts to deprotonate the hydroxo and amido complexes to give oxo and imido complexes were mostly unsuccessful. We now report the synthesis of Ni(II), Pd(II), and Pt(II) diimine supported complexes with oxo or imido ligands both by deprotonation of hydroxo and amido complexes and by oxo–chloro exchange using the gold oxo complex $[(Ph_3PAu)_3(\mu\text{-}O)]^+$.

Results and discussion

Oxo complexes by deprotonation

The dihydroxo complexes $[(Bian)Pt(\mu\text{-}OH)]_2(BF_4)_2$ (Bian = bis(3,5-diisopropylphenylimino)acenapthene) and $[(Bu^t_2bpy)Pt(\mu\text{-}OH)]_2(BF_4)_2$ (Bu^t_2bpy = 4,4′-di-*tert*-butyl-2,2′-bipyridine) undergo facile single deprotonation with stoichiometric or excess 1,8-bis(dimethylamino)naphthalene (Scheme 1). The resulting hydroxo-oxo complexes are isolated as purple (**1**) or red (**2**) salts. (Complex **2** was previously incorrectly reported as a dioxo complex.[29]) The same products are obtained when NaH (**2**) or KOH (**1**) are used as the base and these are preferred for clean isolation of the complexes. Treatment of $[(Bu^t_2bpy)Pd(\mu\text{-}OH)]_2(BF_4)_2$ with NaH gives a yellow complex that is believed to be $[(Bu^t_2bpy)_2Pd_2(\mu\text{-}OH)(\mu\text{-}O)]BF_4$, the Pd analog of **2**. However, characterization is limited to ^1H NMR spectroscopy and elemental analysis and this assignment must be considered tentative especially considering the rarity of Pd oxo complexes.[30–34]

It should be noted that previous attempts to deprotonate $[(Bian)Pt(\mu\text{-}OH)]_2(BF_4)_2$ with $LiN(SiMe_3)_2$ and $KOBu^t$ gave complex mixtures[28] and that deprotonation of phosphine analogs, $[L_2Pt(\mu\text{-}OH)]_2^{2+}$ (L = a phosphine or L_2 = a diphosphine) require much stronger bases. While pK_{a1} in DMSO for these phosphine complexes is only known to be less than 18, a value of 11.9 ± 0.1 for related $[(L_2Pt)_2(\mu\text{-}OH)(\mu\text{-}NMePh)]^{2+}$ (L_2 = dppe) has been measured.[35] The pK_a for singly protonated 1,8-bis(dimethylamino)naphthalene in DMSO is reported as 7.5.[36,37]

[a]*125 Chemistry, University of Missouri, Columbia, Missouri, 65211, USA. E-mail: sharpp@missouri.edu*
[b]*Dipartimento di Chimica, Università di Sassari, Via Vienna 2, I-07100, Sassari, Italy*

† CCDC reference numbers 663517–663527. For crystallographic data in CIF or other electronic format see DOI: 10.1039/b715663d

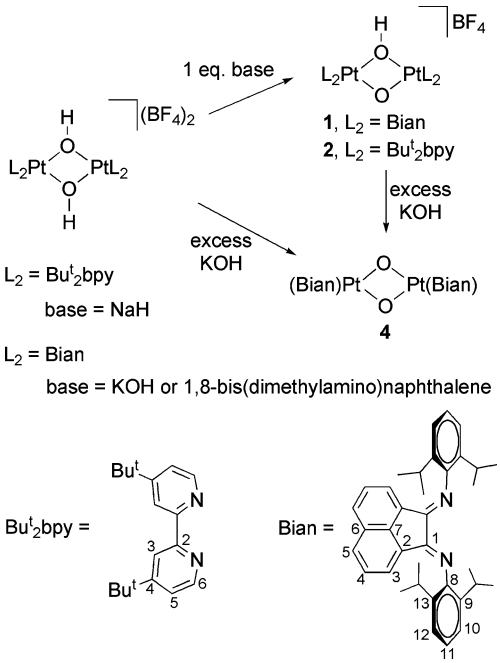

Scheme 1

Assuming that there is no large change in the relative basicities in CH_2Cl_2 then pK_{a1} for $[(Bian)Pt(\mu\text{-}OH)]_2(BF_4)_2$ and $[(But_2bpy)Pt(\mu\text{-}OH)]_2(BF_4)_2$ must be less than 7.5 in DMSO, many units lower than the analogous phosphine complexes. This is consistent with the weaker donor properties of the diimine ligands as compared to the phosphine ligands. We also note that the UV-Vis absorption spectrum of $[(But_2bpy)_2Pt_2(\mu\text{-}OH)(\mu\text{-}O)]BF_4$ (**2**) is essentially identical to that of the complex formulated as $[(bpy)_2Pt_2(\mu\text{-}OH_3)]^+$, produced by increasing the pH of an aqueous solution of $[(bpy)_2Pt_2(\mu\text{-}OH)_2]^{2+}$ to above 8.[38] We therefore propose that $[(bpy)_2Pt_2(\mu\text{-}OH)_3]^+$ be reformulated as $[(bpy)_2Pt_2(\mu\text{-}OH)(\mu\text{-}O)]^+$, the water soluble bpy analog of **2**.

^{1}H NMR spectra of isolated **1** often show broad peaks, which sharpen on addition of 1,8-bis(dimethylamino)naphthalene suggesting that the broadening is associated with proton exchange with trace acidic impurities. The spectra show the expected asymmetry in the Bian ligand with peaks observed for half the Bian ligand on the hydroxo side and peaks for the other half on the oxo side of the complex. Only two peaks are observed for the isopropyl methyl groups indicating that the structure is either planar with the OH group in the plane or if non-planar inverting rapidly on the NMR time scale. An X-ray crystal structure determination on a crystal of **1** grown from CD_2Cl_2–Et_2O was conducted. The crystals contain two crystallographically independent cations each located on an inversion center requiring disorder of the oxo and hydroxo ligands and averaging of the Pt–O bond distances. This and poor quality eliminate much of the significance of the structure other than to confirm the connectivity.

The ^{1}H NMR spectra at 25 °C for **2** are broad and show only one signal for each type of But_2bpy protons suggesting rapid proton exchange between the hydroxo and oxo ligands. At −70 °C (M = Pt) the spectrum is also broad but is resolved into a pattern expected for non-exchanging **2** with two signals for each type of But_2bpy proton. The resonance for one of the But_2bpy H-6 protons at 10.00 ppm is at significantly higher frequency than for the other H-6 proton at 8.68 ppm. This strong shift to higher frequency for one of the But_2bpy H-6 protons is attributed to weak hydrogen interactions with the oxo ligand (Fig. 1). A similar shift is observed in the analogous amido oxo complex **14** (see below).

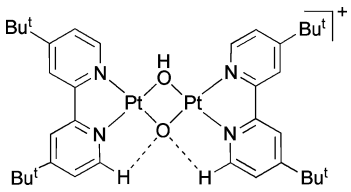

Fig. 1 Drawing of the cationic portion of **2** showing proposed hydrogen interactions.

Confirmation of the hydroxo-oxo formulation for **2** is obtained from the reaction of **2** with MeOTf which yields yellow hydroxo-methoxo complex $[(But_2bpy)_2Pt_2(\mu\text{-}OH)(\mu\text{-}OCH_3)](BF_4)(OTf)$ (**3**, eqn (1)). ^{1}H NMR spectra for **3** show the OMe peak at 3.12 ppm and the OH peak at 4.21 ppm. The two But_2bpy H-6 proton signals appear at similar positions (8.72 and 8.68 ppm) consistent with loss of the hydrogen interaction on methylation of the oxo ligand.

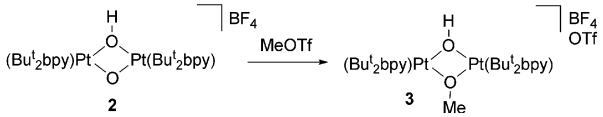

(1)

Deprotonation of the remaining OH group in **1** is possible. If the reaction mixture containing **1** and excess KOH is stirred for prolonged periods (*ca.* 2 h) the mixture becomes deep blue and dark blue dioxo complex $[(Bian)Pt(\mu\text{-}O)]_2$ (**4**) is isolated (Scheme 1). ^{1}H NMR spectra for **4** show a single peak for each type of Bian ligand proton indicative of a planar *mmm*-symmetric structure. Again, peaks are often broadened from protic impurities but sharpen when solid KOH is added to the solution. Attempts to further characterize **4** by X-ray diffraction were thwarted by an inability to isolate suitable crystals. The preparation of derivatives of **4** was therefore undertaken.

"Ph_3PAuBF_4" (prepared from Ph_3PAuCl and $AgBF_4$) addition to a stirred blue solution of **4** results in a dark purple solution of $[(Bian)_2Pt_2(\mu\text{-}O)(\mu\text{-}OAuPPh_3)](BF_4)$ (**5**) (Scheme 2). A crystal of **5** was subjected to a single crystal X-ray structure analysis. Crystal data and data parameters are listed in Table 1. Selected distances and angles are listed in Table 2. A drawing of the solid-state structure of the cationic portion is given in Fig. 2. The Ph_3PAu^+ fragment is bonded to one of the oxo ligands approximately perpendicular to the Pt_2O_2 diamond core reducing the *mmm* symmetry of **4** to *m* symmetry for **5**. Relatively short Au–Pt distances suggest closed-shell interactions between the metal centers.[39,40]

The ^{31}P NMR spectrum for **5** shows the expected singlet (23 ppm) but the ^{1}H NMR spectrum displays only one peak (as opposed to the two predicted from the X-ray structure) for each type of proton in the acenaphthylene portion of the Bian ligand. Similarly, while the X-ray structure predicts 8 signals for the Bian isopropyl methyl groups and 4 signals for the isopropyl CHs only half this number is observed. These data indicate effective *mm* symmetry. This could come about if, in solution, the Ph_3PAu^+ fragment is either bridging between the two oxo ligands or rapidly exchanging (on the NMR time scale) between the two oxo sites.

Table 1 Crystallographic and data collection parameters for $[(Bian)_2Pt_3(\mu_3\text{-}O)(\mu_3\text{-}OAuPPh_3)](BF_4)$ (**5**), $[(Bian)(COD)_2Pt_3(\mu\text{-}OH)_3](OTf)_3$ (**7**), $[(Bu^t_2bpy)_3Ni_3(\mu_3\text{-}O)_2](BF_4)_2$ (**8**), $[(Bu^t_2bpy)Pt(\mu_3\text{-}O)(AuPPh_3)]_2(BF_4)_2$ (**9b**), $[(Bu^t_2bpy)Pd(\mu\text{-}NHAr)]_2(BF_4)_2$ (**12**, Ar = Ph), $[(Bu^t_2bpy)Pd(\mu\text{-}NHAr)]_2(BF_4)_2$ (**12**, Ar = 4-tol), $(Bu^t_2bpy)Pd(OTf)_2$ (**16**), $[(Bu^t_2bpy)Pt(H_2O)_2](OTf)_2$ (**17**) and $[(Bu^t_2bpy)Pt(H_2O)_2](OTf)_2\cdot Et_2O$ (**17**·Et_2O)[a]

	5	**7**	**8**	**9b**	**12** (Ar = Ph)	**12** (Ar = 4-tol)	**16**	**17**	**17**·Et_2O
Formula	$C_{90}H_{95}AuBF_4N_4O_2PPt_2\cdot 0.5CH_2Cl_2\cdot 3.5C_7H_8$[d]	$C_{55}H_{67}F_9N_2O_{12}Pt_3S_3\cdot CH_2Cl_2$	$C_{78}H_{120}B_2F_8N_6Ni_3O_8$	$C_{72}H_{78}Au_2B_2F_8N_4O_2P_2Pt_2\cdot 2(CH_2Cl_2)$	$C_{48}H_{60}B_2F_8N_6Pd_2\cdot 4C_4H_8O$	$C_{50}H_{64}B_2F_8N_6Pd_2\cdot 4CH_2Cl_2$	$C_{20}H_{24}F_6N_2O_6PdS_2$	$C_{20}H_{28}F_6N_2O_8PtS_2$	$C_{20}H_{28}F_6N_2O_8PtS_2\cdot C_4H_{10}O$
fw	2330.56	1885.48	1619.55	2220.91	1395.86	1475.20	672.93	797.65	871.77
Space group	$P2_1/n$	$P\bar{1}$	$P4_2/ncm$	$P2_1/c$	$P2_1/n$	$P2_1/c$	C_2/c	$P2_1/n$	$P\bar{1}$
a/Å	13.8799(14)	14.1910(10)	18.8011(11)	13.5140(7)	17.4761(8)	11.627(4)	24.7290(12)	9.5825(5)	11.6959(8)
b/Å	31.125(3)	14.2422(10)	18.8011(11)	15.3931(8)	11.1520(5)	24.551(8)	14.0562(7)	10.9866(6)	12.3527(9)
c/Å	25.166(3)	17.7064(13)	25.787(3)	18.8441(10)	18.0618(8)	11.490(4)	19.0437(9)	27.0029(13)	13.1273(9)
α/deg	90	93.3520(10)	90	90	90	90	90	90	92.1490(10)
β/deg	104.968(2)	92.0490(10)	90	96.2570(10)	109.2730(10)	77.461(5)	127.647(1)	90.5780(10)	113.6370(10)
γ/deg	90	117.1220(10)	90	90	90	90	90	90	104.7530(10)
V/Å^3	10503.3(18)	3171.8(4)	9115.3(13)	3896.6(4)	3322.8(3)	3201.8(17)	5241.3(4)	2842.7(3)	1659.2(2)
Z	4	2	4	2	2	2	8	4	2
d_{calc}/g cm^{-3}	1.497	1.974	1.180	1.893	1.395	1.530	1.706	1.864	1.745
μ/mm^{-1}	4.175	6.869	0.680	7.576	0.613	0.959	0.948	5.167	4.436
$R1$, [b] $wR2$[c]	0.0476, 0.1028	0.0491, 0.0982	0.0759, 0.2174	0.0340, 0.0786	0.0380, 0.0866	0.0412, 0.0996	0.0264, 0.0653	0.0426, 0.0835	0.0231, 0.0560

[a] λ = 0.71070 Å (Mo), $T = -100$ °C. [b] $R1 = (\Sigma \| F_o \| - \| F_c \|)/\Sigma | F_o |$. [c] $wR2 = [(\Sigma w(F_o^2 - F_c^2)^2)/\Sigma w(F_c^2)^2]^{1/2}$. [d] Idealized toluene.

Table 2 Selected distances and angles for $[(Bian)_2Pt_2(\mu\text{-}O)(\mu\text{-}OAuPPh_3)]BF_4$ (**5**)

Au1–O1	2.054(5)	Au1–Pt1	3.0494(5)
Au1–P1	2.218(2)	Au1–Pt2	3.1949(5)
Pt1–O1	2.021(5)	Pt2–O1	2.023(5)
Pt1–O2	1.961(5)	Pt2–O2	1.972(5)
Pt1–N1	2.018(6)	Pt2–N3	2.009(6)
Pt1–N2	1.993(7)	Pt2–N4	2.007(6)
O1–Au1–P1	176.24(15)	Pt1–Au1–Pt2	56.626(10)
O2–Pt1–N2	97.8(3)	O2–Pt2–N4	101.4(2)
O2–Pt1–N1	174.4(2)	O2–Pt2–N3	175.1(2)
N1–Pt1–N2	79.3(3)	N4–Pt2–N3	80.1(3)
O2–Pt1–O1	80.4(2)	O2–Pt2–O1	80.1(2)
N1–Pt1–O1	103.3(2)	N3–Pt2–O1	99.1(2)
N2–Pt1–O1	170.6(2)	N4–Pt2–O1	172.3(2)
Pt1–O1–Au1	96.9(2)	Pt1–O1–Pt2	94.3(2)
Pt2–O1–Au1	103.2(2)	Pt1–O2–Pt2	97.8(2)

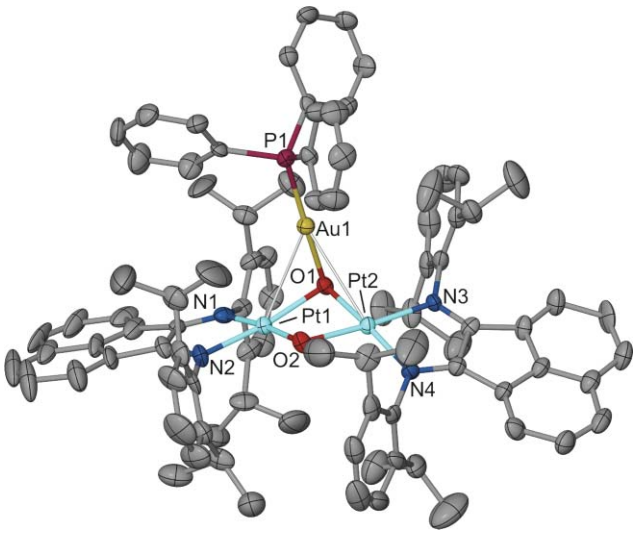

Fig. 2 Drawing (50% probability ellipsoids) of the cationic portion of the solid-state structure of $[(Bian)_2Pt_2(\mu\text{-}O)(\mu\text{-}OAuPPh_3)]BF_4$ (**5**).

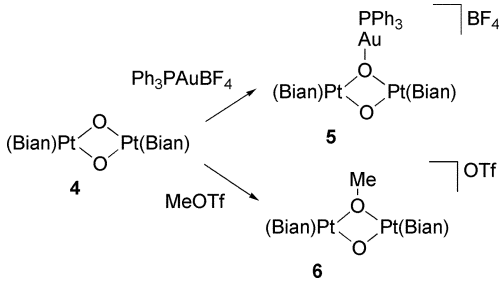

Scheme 2

Interestingly, when the probe temperature is raised to 25 °C the ^{31}P NMR peak broadens, as do the ^1H NMR signals for the Bian isopropyl groups. The ^1H NMR signals for the Bian acenaphthylene unit remain sharp. This broadening is apparently due to exchange of the Ph_3PAu^+ fragment with trace amounts of Ph_3PAuCl that is visible in the low temperature ^{31}P NMR spectra (33 ppm) but not in the room temperature spectrum. Given the crowded structure of **5** (see below) the exchange is attributed to Ph_3PAu^+ dissociation from **5**.

Addition to the oxo ligand of **4** is also observed when MeOTf is added to solutions of **4** and dark purple [(Bian)$_2$Pt$_2$(μ-O)(μ-OMe)]OTf (**6**) is isolated. A crystal structure determination on a crystal of **6** confirms the connectivity but the structure is of poor quality with badly disordered solvent molecules and triflate anion.

As in **5**, ^{1}H NMR data for **6** are inconsistent with the *m* symmetry of the solid-state structure. Two signals (overlapping) for each type of proton in the acenaphthylene portion of the Bian ligand are observed but only 4 signals for the Bian isopropyl methyl groups and 2 signals for the isopropyl CHs are present. We attribute this higher apparent symmetry to rapid inversion at the methoxo ligand oxygen atom effectively producing mirror symmetry around the Pt_2O_2 plane. The methoxo methyl group signal is observed at 2.48 ppm. The reaction of **4** with excess MeOTf was investigated and gave a red product that is likely (Bian)Pt(OTf)$_2$. However, this product was not completely characterized (see Experimental).

Treatment of a blue solution of **4** with Pt(COD)(OTf)$_2$ first gives a purple solution but this changes to yellow-brown. A brown solid is isolated that by ^{1}H NMR spectroscopy shows a symmetric environment for the Bian ligand and a Pt-bonded COD ligand in about a 1 : 1 ratio. Recrystallization yielded a small amount of orange-red crystals, which were identified by an X-ray diffraction analysis as the hydroxo bridged complex [(Bian)Pt$_3$(μ-OH)$_3$(COD)$_2$] (OTf)$_3$ (**7**) (Fig. 3, eqn (2)). Crystal data and data parameters are listed in Table 1. Selected distances and angles are given in Table 3. The H$^+$ source is unknown but is presumably from trace water in the reaction system. Related complexes with a Pt$_3$(μ-OH)$_3$ core have been reported.[41–45]

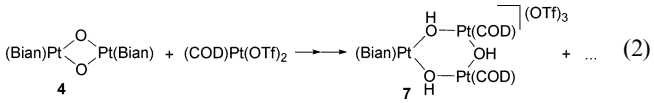

(2)

Oxo complexes by chloro–oxo exchange

We have previously reported the use of the Au oxo complex [(Ph$_3$PAu)$_3$(μ-O)]BF$_4$ as an oxide ion source in exchange reactions with [M(diene)(μ-Cl)]$_2$ (M = Rh, Ir),[46] (COD)PtCl$_2$,[47] (DBCOT)PtCl$_2$ (DBCOT = dibenzo[*a*,*e*]cyclooctatetraene)[48] and (Bu$^t_2$bpy)PdCl$_2$[30] and find it effective here for Ni(II) and Pt(II) chloro complexes. Thus, mixing Ni(Bu$^t_2$bpy)Cl$_2$ with [(Ph$_3$PAu)$_3$(μ-O)]BF$_4$ in a 3 : 2 ratio in CH$_2$Cl$_2$ yields the red oxo complex [Ni$_3$(Bu$^t_2$bpy)$_3$(μ-O)$_2$](BF$_4$)$_2$ (**8**) and Ph$_3$PAuCl (eqn (3)).

Table 3 Selected distances and angles for [(Bian)(COD)$_2$Pt$_3$(μ-OH)$_3$](OTf)$_3$ (**7**)

Pt1–O1	2.001(6)	Pt1–N1	2.004(7)
Pt1–O2	2.003(6)	Pt1–N2	2.019(7)
Pt2–O2	2.047(6)	Pt3–O1	2.040(6)
Pt2–O3	2.064(6)	Pt3–O3	2.080(6)
Pt2–C41	2.123(9)	Pt3–C50	2.136(10)
Pt2–C42	2.130(9)	Pt3–C46	2.136(10)
Pt2–C38	2.156(9)	Pt3–C49	2.141(9)
Pt2–C37	2.161(9)	Pt3–C45	2.152(9)
O1–Pt1–O2	88.3(2)	O1–Pt1–N2	175.3(3)
O1–Pt1–N1	94.8(3)	O2–Pt1–N2	95.7(3)
O2–Pt1–N1	176.8(3)	N1–Pt1–N2	81.2(3)
O2–Pt2–O3	92.4(2)	O1–Pt3–O3	90.0(2)
Pt1–O1–Pt3	126.9(3)	Pt2–O3–Pt3	131.1(3)
Pt1–O2–Pt2	123.1(3)		

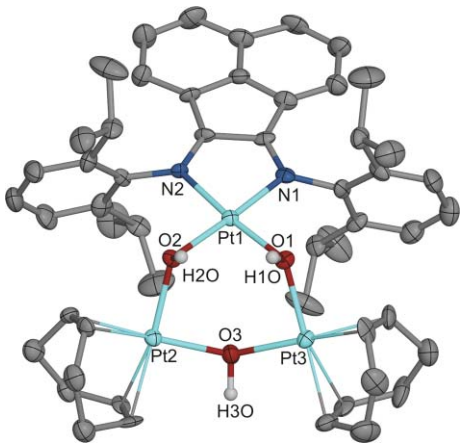

Fig. 3 Drawing (50% probability ellipsoids) of the cationic portion of the solid-state structure of [(Bian)Pt$_3$(μ-OH)$_3$(COD)$_2$] (OTf)$_3$ (**7**).

Table 4 Selected distances and angles for [(Bu$^t_2$bpy)$_3$Ni$_3$(μ-O)$_2$](BF$_4$)$_2$ (**8**)[a]

Ni1–O1	1.852(4)	Ni1–N1	1.880(5)
Ni2–O1	1.845(3)	Ni2–N2	1.874(4)
Ni1–Ni2	2.4816(12)	Ni2–Ni2*	2.5488(15)
N1–Ni1–N1*	84.8(3)	N2–Ni2–N2	84.3(2)
O1–Ni1–O1*	76.7(3)	O1–Ni2–O1*	77.1(2)
O1–Ni1–N1	99.2(2)	O1–Ni1–N1*	176.0(2)
O1–Ni2–N2	99.27(15)	O1–Ni2–N2*	175.51(17)
Ni2–O1–Ni2*	87.37(18)	Ni2–O1–Ni1	84.33(15)

[a] Atoms with an asterisk are related to unmarked atoms by inversion.

A drawing of the cationic portion of the solid-state structure of **8** is given in Fig. 4. Crystal data and data parameters are listed in Table 1. Selected distances and angles are listed in Table 4. The core structure consists of a triangle of Ni atoms bicapped by the oxo ligands. ^{1}H NMR data are in agreement with the solid-state structure showing a single set of signals for a symmetric Bu$^t_2$bpy ligand.

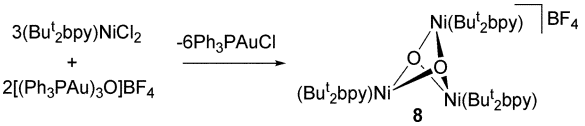

(3)

Treatment of Ni(Bu$^t_2$bpy)Cl$_2$ with 1 equiv of [(Ph$_3$PAu)$_3$(μ-O)]BF$_4$ gives a product different from **8** by ^{31}P NMR spectroscopy. Attempts to isolate this product yielded only **8**. In analogy to the Pd and Pt chemistry that follows this product is believed to be [Ni(Bu$^t_2$bpy)(μ-OAuPPh$_3$)]$_2$(BF$_4$)$_2$. Its instability relative to **8** and the analogous Pt and Pd complexes is attributed to the greater oxophilicity expected for the more electropositive Ni center.

In contrast to Ni, Pt(Bu$^t_2$bpy)Cl$_2$ and [(Ph$_3$PAu)$_3$(μ-O)]BF$_4$ gives only the mixed Pt–Au oxo complexes [M(Bu$^t_2$bpy)(μ-OAuPPh$_3$)]$_2$(BF$_4$)$_2$ (**9**, M = Pt, Scheme 3). We previously reported the analogous reaction with Pd(Bu$^t_2$bpy)Cl$_2$ that gives the Pd analog **9** (M = Pd).[30] Both the Pd and Pt derivatives have now been structurally characterized by X-ray diffraction. The crystals are isomorphous and the complexes are isostructural. Crystal data and data parameters are listed in Table 1. Selected distances and angles for the Pt structure are listed in Table 5 and a drawing of

Table 5 Selected Distances and Angles for $[(Bu^t_2bpy)Pt(\mu\text{-}OAuPPh_3)]_2(BF_4)_2$ (**9b**)[a]

Pt1–O1	2.034(3)	Au1–O1	2.057(3)
Pt1–O1*	2.017(3)	Au1–P1	2.2170(15)
Pt1–N1	1.996(4)	Au1–Pt1	2.9937(3)
Pt1–N2	1.994(4)	Au1–Pt1*	3.2600(3)
Pt1–Pt1*	3.0642(4)		
Pt1–Au1–Pt1*	58.493(8)	O1–Au1–P1	171.91(10)
N1–Pt1–N2	80.63(18)	N2–Pt1–O1*	98.06(16)
N1–Pt1–O1*	177.60(15)	N2–Pt1–O1	177.42(16)
N1–Pt1–O1	99.50(16)	O1–Pt1–O1*	81.71(15)
Pt1–O1–Au1	94.06(14)	Pt1–O1–Pt1*	98.29(15)
Pt1–O1–Au1*	106.31(16)		

[a] Atoms with an asterisk are related to unmarked atoms by inversion.

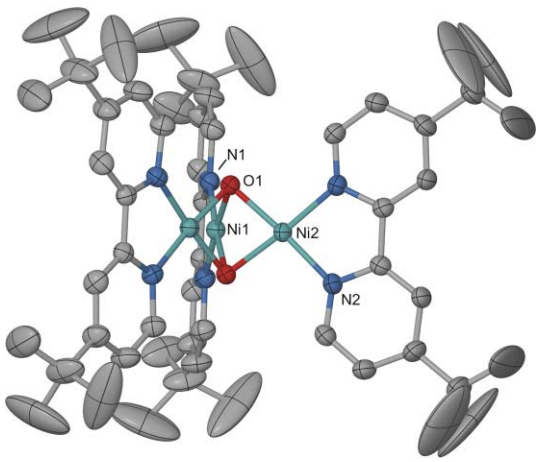

Fig. 4 Drawing (50% probability ellipsoids) of the cationic portion of the solid-state structure of $[Ni_3(Bu^t_2bpy)_3(\mu\text{-}O)_2](BF_4)_2$ (**8**). Mirrors in the Ni1, O1, N1 and the Ni atom plane relate labeled and unlabeled atoms.

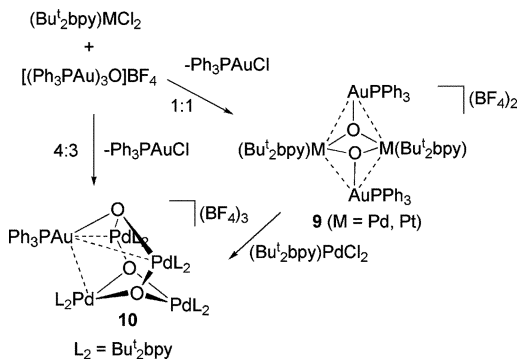

Scheme 3

the cationic portion is given in Fig. 5. Data for the Pd complex have been previously reported.[30]

The cationic portion consists of an inversion symmetric dimer containing a planar M_2O_2 diamond core with a Ph_3PAu group bonded to each oxo ligand. The Ph_3PAu groups are oriented approximately perpendicular to the diamond plane in *anti*-positions with respect to one another. NMR spectra for **9** suggest the same structure in solution. A singlet for the $AuPPh_3$ group is observed at 25.5 (M = Pt) and 26.6 (M = Pd) ppm in the ^{31}P NMR spectra. ^1H NMR spectra show a symmetric pattern for the Bu^t_2bpy ligand with a single Bu^t resonance.

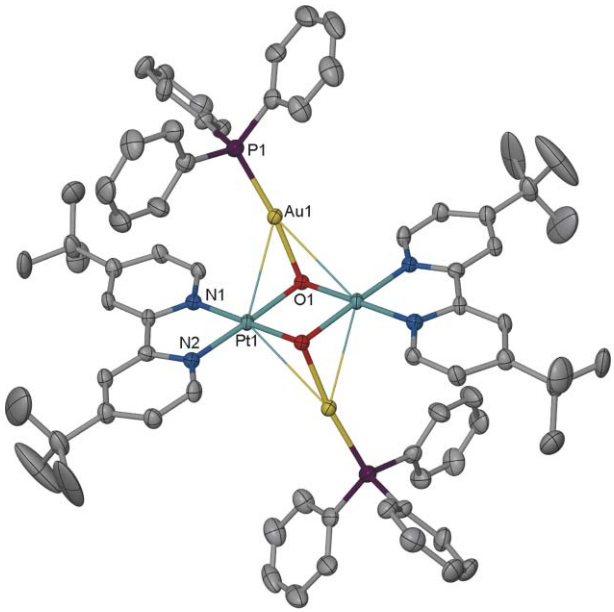

Fig. 5 Drawing (50% probability ellipsoids) of the inversion-centered cationic portion of the solid-state structure of $[Pt(Bu^t_2bpy)(\mu\text{-}OAuPPh_3)]_2(BF_4)_2$ (**9**, M = Pt).

Altering the 1 : 1 reactant ratio in the reaction of $M(Bu^t_2bpy)Cl_2$ with $[(Ph_3PAu)_3(\mu\text{-}O)]BF_4$ does not change the identity of the reaction products when M = Pt. However, as previously reported, with M = Pd the new oxo complex $[Pd_4(Bu^t_2bpy)_4(\mu\text{-}OAuPPh_3)](BF_4)_3(\mu\text{-}O)_2$ (**10**) is obtained (Scheme 3). Addition of $Pd(Bu^t_2bpy)Cl_2$ to **9** also yields **10**. The lack of formation of a similar complex for Pt is presumably kinetic.

Amido and imido complexes

A well-established method for the synthesis of late transition metal amido complexes is by the reaction of amines, particularly aryl amines, with hydroxo complexes (for recent examples, see references 35,49–51). This is an effective method with the Bu^t_2bpy complexes but the final product depends on the metal and the reaction conditions (Scheme 4). (Similar behavior is observed for analogous phosphine complexes.[52]) Treatment of the Pt dihydroxo complex $[Pt(Bu^t_2bpy)(\mu\text{-}OH)]_2(BF_4)_2$ with 4 equivalents of $ArNH_2$ yields the amido hydroxo complexes $[Pt_2(Bu^t_2bpy)_2(\mu\text{-}NHAr)(\mu\text{-}OH)](BF_4)_2$ (**11**, Ar = Ph, 4-tol, 4-$C_6H_4NO_2$). Under the same conditions the Pd dihydroxo complex $[Pd(Bu^t_2bpy)(\mu\text{-}OH)]_2(BF_4)_2$ yields the diamido complexes $[Pd(Bu^t_2bpy)(\mu\text{-}NHAr)]_2(BF_4)_2$ (**12**, Ar = Ph, 4-tol, 4-$C_6H_4NO_2$). The analogous Pt diamido complex $[Pt(Bu^t_2bpy)(\mu\text{-}NH(4\text{-}tol))]_2(BF_4)_2$ (**13**) is obtained by further treatment of **11** (Ar = 4-tol) with 4-toluidine. Complexes **11** and **12** are also formed from the dihydroxo complexes and LiNHAr. The difference between the Pt and Pd chemistry is attributed to the greater kinetic reactivity of a second row transition metal as compared to a third row transition metal, a well-known phenomenon.[53]

Solid-state X-ray crystal structure determinations (Tables 1 and 6) on **12** (Ar = Ph, 4-tol) reveal retention of the diamond core with slight deviations from planarity. A drawing of the structure of **12** (Ar = Ph) is given in Fig. 6. The aryl rings are found to be in an

Table 6 Selected distances and angles for $[(Bu^t_2bpy)Pd(\mu\text{-}NHAr)]_2(BF_4)_2$ (**12**, Ar = Ph, 4-tol)[a]

	Ar = Ph	Ar = 4-tol
Pd1–N1	2.024(2)	2.034(3)
Pd1–N2	2.045(2)	2.039(3)
Pd1–N3	2.047(2)	2.055(2)
Pd1–N3*	2.053(2)	2.053(3)
Pd1–Pd1*	3.1099(4)	3.1015(8)
N3–C(*ipso*)	1.428(4)	1.434(4)
N1–Pd1–N2	79.77(9)	79.89(10)
N1–Pd1–N3	176.29(11)	175.83(10)
N1–Pd1–N3*	98.81(10)	98.64(10)
N2–Pd1–N3	100.45(10)	99.85(10)
N2–Pd1–N3*	174.58(11)	175.11(10)
N3–Pd1–N3*	81.31(11)	81.96(10)
C(*ipso*)–N3–Pd1	113.49(19)	113.38(18)
C(*ipso*)–N3–Pd1*	113.3(2)	111.70(18)
Pd1–N3–Pd1*	98.69(11)	98.04(10)

[a] Atoms with an asterisk are related to unmarked atoms by inversion.

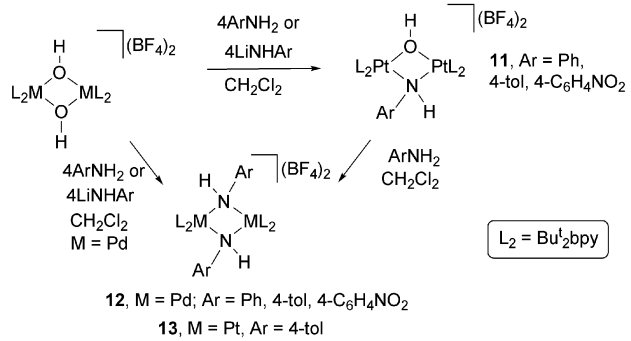

Scheme 4

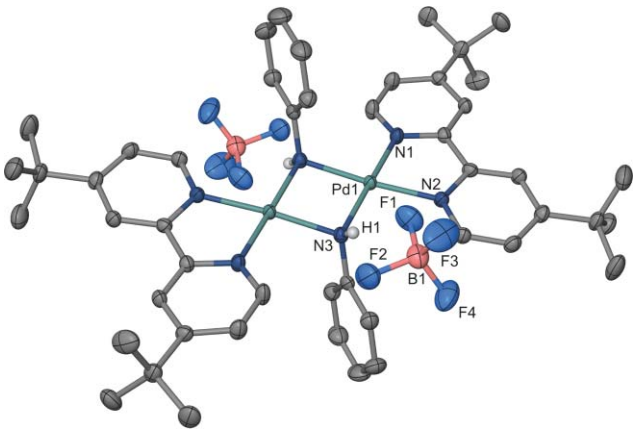

Fig. 6 Drawing (50% probability ellipsoids) of the solid-state structure of $[Pd(Bu^t_2bpy)(\mu\text{-}NHPh)]_2(BF_4)_2$ (**12**, Ar = Ph). Labeled and unlabeled atoms are related by an inversion center.

anti-orientation across the diamond core in both structures with the BF_4 anions hydrogen bonded to the amido hydrogen atoms.

Solution ^1H NMR data for **11**, **12**, and **13** are consistent with the assigned structures. Two sets of resonances for each type of proton on the Bu^t_2bpy ligand are observed for **11** and resonances for the OH and NH groups are observed at 5.17 and 2.25 ppm for Ar = Ph and 5.20 and 2.55 ppm for Ar = *p*-tol. The higher shift resonance in each set is assigned to the NH group. Complexes **12** and **13** show only one resonance for each type of proton on the Bu^t_2bpy ligand consistent with high symmetry of the dication. The NH signals are observed at 2.83 (Ar = 4-tol), 2.89 (Ar = Ph), and 3.54 (Ar = 4-$NO_2C_6H_4$) ppm for **12**. A larger N–H shift of 4.97 ppm is observed for **13** and is similar to the N–H shifts in **11**. Larger N–H and O–H shifts for Pt over the Pd complexes are probably related to a greater acidity for the Pt complexes.

Amido-oxo and diimido complexes

Deprotonation of amido hydroxo **11** (Ar = 4-tol) is accomplished with either NaH or 1,8-bis(dimethylamino)naphthalene yielding the orange amido oxo complex $[Pt_2(Bu^t_2bpy)_2(\mu\text{-}NH\text{-}tol\text{-}4)(\mu\text{-}O)]BF_4$ (**14**, Scheme 5). As with the dihydroxo complexes (see above) deprotonation with 1,8-bis(dimethylamino)naphthalene indicates a DMSO pK_a for **14** that is under 7.5, the pK_a of 1,8-bis(dimethylamino)naphthalene in DMSO.[36,37] This is considerably less than the pK_a (11.9) for the diphosphine analog $[(L_2Pt)_2(\mu\text{-}OH)(\mu\text{-}NMePh)]^{2+}$ (L_2 = dppe).[35] Complex **14** is also obtained when $[Pt(Bu^t_2bpy)(\mu\text{-}OH)]_2(BF_4)_2$ is refluxed in THF with 4 equivalents of toluidine contrasting sharply to the formation of amido-hydroxo **11** in CH_2Cl_2 (see above). The ^1H NMR spectrum for **14** is very similar to that of **11** (Ar = 4-tol) with two exceptions. A signal for an OH group is absent and the resonance for one of the Bu^t_2bpy H-6 protons is strongly shifted from 8.78 to 10.28 ppm. The shift to higher frequency is attributed to interactions between the Bu^t_2bpy H-6 protons and the new oxo ligand (see Scheme 5) similar to what is observed for the analogous hydroxo-oxo complex **2** (see above). Unfortunately, crystals for an X-ray analysis, which could possibly confirm the interaction, could not be obtained.

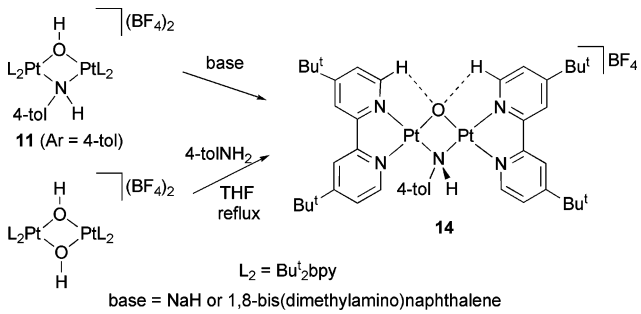

Scheme 5

Treatment of diamido **13** with $KOBu^t$ in CH_2Cl_2 gives a deep green complex, which we have assigned as the neutral diimido complex $[Pt(Bu^t_2bpy)(\mu\text{-}N\text{-}4\text{-}tol)]_2$ **15** (eqn (4)). No ^1H NMR signal for an N–H group could be detected and the signals for the N–Ar ligand and the Bu^t_2bpy ligands indicate a symmetric structure. While there is a slight shift of the Bu^t_2bpy H-6 protons to higher frequency on deprotonation (from 8.47 ppm in **13** to 9.06 ppm in **15**) there is not the dramatic shift indicative of the hydrogen atom interactions observed for oxo complexes **2** and **14**. This is likely due to a blocking effect of the 4-tol group on the imido nitrogen atom.

Table 7 Selected distances and angles for (Bu^t_2bpy)Pd($OTf)_2$ (**16**)

Pd1–N2	1.9715(17)	Pd1–O1	2.0503(15)
Pd1–N1	1.9815(16)	Pd1–O4	2.0589(14)
N2–Pd1–N1	81.31(7)	N2–Pd1–O4	95.00(6)
N2–Pd1–O1	174.27(6)	N1–Pd1–O4	173.92(7)
N1–Pd1–O1	92.99(6)	O1–Pd1–O4	90.72(6)

Table 8 Selected distances and dngles for [(Bu^t_2bpy)Pt($H_2O)_2$]($OTf)_2$ (**17**), and [(Bu^t_2bpy)Pt($H_2O)_2$]($OTf)_2$·Et_2O (**17**·Et_2O)

	17	**17**·Et_2O
Pt1–N2	1.966(5)	1.974(3)
Pt1–N1	1.974(5)	1.982(2)
Pt1–O2	2.049(5)	2.038(2)
Pt1–O1	2.052(5)	2.043(2)
N2–Pt1–N1	81.1(2)	81.52(10)
N2–Pt1–O2	94.5(2)	93.37(10)
N1–Pt1–O2	175.1(2)	174.78(10)
N2–Pt1–O1	173.8(2)	175.87(9)
N1–Pt1–O1	94.9(2)	94.51(10)
O2–Pt1–O1	89.67(19)	90.61(10)

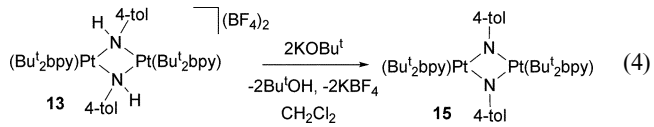

(4)

Triflate and aqua[54] complexes

During the course of this investigation the triflate complexes (Bu^t_2bpy)M($OTf)_2$ (**16**, M = Pd, Pt) were prepared (Scheme 6). The Pt complex has been previously prepared in an identical manner,[55] as have closely related triflate complexes.[56,57] An X-ray crystal structure determination of the Pd derivative (Tables 1 and 7) confirmed the identity of the complex and shows bonding of the triflate anions to the Pt center. A drawing of the molecule is provided in Fig. 7. The triflate anions are readily displaced from the Pt center of **16** (M = Pt) by water yielding the dicationic aqua complex [Pt(Bu^t_2bpy)($H_2O)_2$]($OTf)_2$ (**17**) (for other diimine Pt aqua complexes see: references 58,59). Unsolvated and ether solvated crystals were isolated and both were subjected to X-ray crystal structure determinations (Tables 1 and 8). A drawing of the unsolvated structure is shown in Fig. 8. The ether solvate is similar except that one of the triflate anions is only hydrogen bonded to one of the water ligands allowing hydrogen bonding of the ether molecule to the other water ligand (see supporting information).

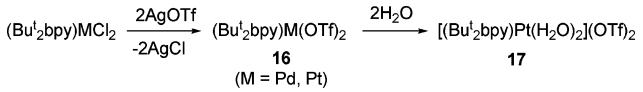

Scheme 6

Structures

All of the Pt and Pd structures, except that of triplatinum complex **7** and the mononuclear complexes **16** and **17**, are based on an M_2X_2 diamond core (M = Pd, Pt; X = N, O). This core for d^8 metals with a variety of X groups has attracted attention for its tendency to be

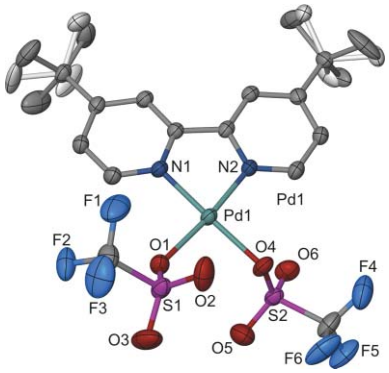

Fig. 7 Drawing (50% probability ellipsoids) of the solid-state structure of Pd(Bu^t_2bpy)($OTf)_2$ (**16**, M = Pd). Rotational disorder observed in the Bu^t groups is illustrated.

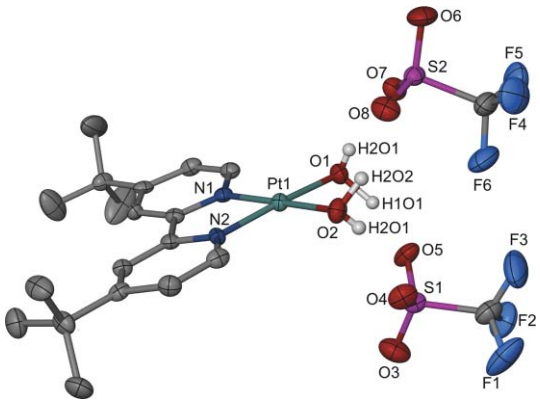

Fig. 8 Drawing (50% probability ellipsoids) of the solid-state structure of the unsolvated form of [Pt(Bu^t_2bpy)($H_2O)_2$]($OTf)_2$ (**17**).

planar, as found for the complexes here, or "bent" by folding along the X–X axis.[60,61] Planarity is promoted by high electronegativity X groups and weak donor ligands on the metal center consistent with the planarity of the structure reported here.

As a result of the similar sizes of Pt and Pd and O and N the M_2X_2 diamond core angles for our complexes are all comparable with M–X–M angles close to 100° and the X–M–X angles at about 80°. These angles fall within the range reported for the many analogous Pt and Pd complexes with this core structure.[62] Three of the complexes reported here are exceptional. Complexes **1**, **5**, and **6** are the first structurally characterized Pt complexes containing truly μ_2-oxo ligands bridging between two Pt centers. Other reported Pt and Pd bridged oxo complexes are μ_3,[21,29,47,52,63–67] or μ_4,[33,68] or if μ_2 are found to be associated with Li salts through coordination of the oxo ligand to an alkali metal ion effectively giving μ_3-oxo complexes.[29,52,69,70] While the disorder between the oxo and hydroxo ligands in **1** and the poor structure quality of **6** do not allow an examination of the structural details of a μ_2-oxo ligand, complex **5** allows an internal comparative analysis of a μ_3-oxo and a μ_2-oxo ligand and this structure will be examined in more detail.

The Au–O distance of 2.054(5) Å in **5** is in the range observed in other Au(I) μ_3-oxo complexes[47,48,71] including **9** (M = Pt). In addition, the Pt–Au distances (3.195 and 3.049 Å) are consistent with d^8–d^{10} closed-shell interactions between the Au and Pt centers. A difference of 0.056 Å between the Pt–O distances for the

μ_3-oxo ligand (average = 2.022 Å) and the μ_2-oxo ligand (average = 1.967(8) Å) suggests a lengthening of this distance on coordination of the Ph_3PAu^+ fragment to the oxo ligand. This is consistent with the well-known phenomenon of increasing bond lengths with increasing atom coordination number.[72] As discussed next, steric interactions may also play a role in the lengthening of the Pt–O distances.

The coordination environment of the Pt centers of **5** is strongly distorted from planarity. This is primarily due to a displacement of the Au bonded oxygen atom O1 out of the Pt coordination planes defined by Pt1, N1, N2, O2 (deviation < 0.06 Å) and Pt2, N3, N4, O2 (deviation < 0.05 Å). The O1 displacement is 0.42 Å for the Pt1 plane and 0.93 Å for the Pt2 plane. This displacement appears to arise from steric interactions of the phenyl rings of the Ph_3PAu^+ fragment with the $Pr^i_2C_6H_3$ groups of the Bian ligand and probably accounts for the facile exchange of the Ph_3PAu^+ fragment with Ph_3PAuCl in solution (see above).

Complex **9** (M = Pt) is related to **5** by replacement of the Bian ligand with a Bu^t_2bpy ligand and by coordination of another Ph_3PAu^+ fragment to the second oxo group. As might be expected, the Pt–O (2.026(12) Å) and Au–O (2.057(3) Å) distances are very similar to those of the μ_3-oxo group in **5**. Again, the steric interactions causing the distortions in **5** are absent in **9** due now to the replacement of the Bian ligand with the less sterically demanding Bu^t_2bpy ligand and the coordination environment of the Pt centers is now essentially planar.

Nickel complex **8** can also be considered to be based on a diamond core where anyone of the three Ni(II) centers may be taken to bridge across the two oxygen atoms of an Ni_2O_2 diamond core. With the smaller sized Ni center the core angles in **8** are reduced to average values of 85.8° (Ni–O–Ni) and 76.9° (O–Ni–O). A more accurate description of the core structure of **8** is that of a trigonal bipyramid or a dioxo bicapped triangle. While this structural motif has been observed before for Ni(II) complexes with an Ni_3O_2 core these have been, with one exception, RO ligand complexes and not oxo ligand complexes.[73–77] The exception is a Ni_6 structure with a single μ_6-oxo ligand bridging two Ni_3OH units.[78] The Ni–O bonds in these complexes range from 1.906(8) to 2.516(5) Å, generally longer than the average value of 1.849 Å in **8**. Oxo ligands are encountered in diatomic Ni(III) complexes with Ni_2O_2 cores. Those that have been structurally characterized show Ni–O bond distances similar to those in **8** (1.841(7), 1.870(8);[15] 1.888(6), 1.854(7);[79] 1.843(5), 1.857(4), 1.76(3), 1.81(2) Å[80]). A single Ni–O–Ni bridge exists in the Ni(III) complex $[Ni(salen)]_2O$. Here the Ni–O distances are shorter than in **8** at 1.790(2) Å.[81] Mixed-metal Ni oxo complexes have also been reported. In the Ni(II) complex $[Ni(acac)_2(PhHgOHgPh)]_2$ the structure consists of a Ni_2O_2 diamond core with two PhHg units coordinated to each oxo group. The Ni–O distance is 2.096(4) Å.[82] [CrFeNiO(OCCH)(py)] metals are disordered.[83] Finally, the Pd and Pt sulfido analogs of **8**[84] and sulfido complexes with Ni_3S_2 trigonal bipyramidal cores with phosphine,[85] allyl,[86] and sulfur[87] ligands have been reported and structurally characterized.

Concluding remarks

Previous work in our group has focused on phosphine ligand supported hydroxo and amido complexes and their deprotonation to oxo and imido complexes. The diimine ligand supported complexes described here show similar features but the facile deprotonation of the hydroxo complexes and the amido complexes indicate that the diimine ligands impart greater acidity to the hydroxo and amido ligands. This apparent greater acidity may be attributed to the reduced metal center electron donation of diimine ligands as compared to phosphine ligands. The reduced metal center electron density allows for a greater M–O interaction and more electron density transfer from the hydroxo or amido ligand to the metal center.

Experimental

Experiments were performed under a dinitrogen atmosphere in a Vacuum Atmospheres Corporation dry box. Solvents were dried by standard techniques and stored under dinitrogen over 4 Å molecular sieves or sodium metal unless otherwise indicated. NMR spectra were recorded at ambient temperatures unless otherwise indicated on a Bruker AMX-250, -300, or -500 spectrometer using external $CFCl_3$ (^{19}F), K_2PtCl_4(aq) (^{195}Pt), and H_3PO_4 (^{31}P) as standards and are reported in ppm with negative shifts to lower frequency of the standard. For ^1H NMR spectra solvent impurities were used to reference back to $SiMe_4$. Labeling of the Bian and Bu^t_2bpy ligands for the NMR assignments is given in Scheme 1. Mass spectra were obtained on a Finnigan TSQ7000 mass spectrometer. Desert Analytics performed the microanalyses (inert atmosphere). The presence of solvent of crystallization in the analyzed samples was confirmed by NMR spectroscopy. $Pd(Bu^t_2bpy)Cl_2$,[88] $Pt(Bu^t_2bpy)Cl_2$,[29] $[(Bu^t_2bpy)Pt(\mu\text{-}OH)]_2(BF_4)_2$,[29] $[(Ph_3PAu)_3(\mu_3\text{-}O)]BF_4$,[89] $(COD)Pt(OTf)_2$[90,91] and $(Bian)PtCl_2$[92] were prepared by literature procedures. Nickel(II) chloride was dried overnight at 100 °C. Other reagents were purchased from commercial sources (Aldrich or Acros) and used as received.

$(Bu^t_2bpy)NiCl_2$

A solution of $NiCl_2$ (200 mg, 1.54 mmol) in absolute ethanol (30.0 mL) was added to a stirred suspension of Bu^t_2bpy (413 mg, 1.54 mmol) in absolute ethanol (30.0 mL). The reaction mixture was refluxed with stirring. Over 5 h the yellow solution slowly became green and a green solid deposited. The green solid product was collected by filtration, washed with hot ethanol and then diethyl ether and then dried at 160 °C for 3 h. Yield: 565.0 mg (92%). The product was recrystallized for analysis from CH_2Cl_2–ether. Anal. calcd (found) for $C_{18}H_{24}N_2NiCl_2$: C, 54.27 (54.15); H, 6.03 (6.13); N, 7.03 (6.87%). ^1H NMR (CD_2Cl_2): The paramagnetic product shows only a broad peak at 1.69 ppm.

$[Pt(\mu\text{-}OH)(Bian)]_2(BF_4)_2$

This complex was prepared by the following modified literature procedure.[28] $(Bian)PtCl_2$ (50 mg, 0.065 mmol) was suspended in 2 mL of THF. $AgBF_4$ (30 mg, 0.015 mmol), a small amount of polyvinyl pyridine, and a drop of water were added. The mixture was refluxed overnight. The volatiles were then removed *in vacuo* and the residue dissolved in 15 mL of CH_2Cl_2. The solution was passed through a pad of diatomaceous earth, reduced in volume

to *ca.* 3 mL, layered with diethyl ether, and cooled to 0°C to obtain dark red needle shaped crystals of the product. Yield: 36 mg (70%).

[(Bu$^t_2$bpy)Pd(μ-OH)]$_2$(BF$_4$)$_2$

Solid $AgBF_4$ (390 mg, 2.00 mmol) and 3–4 drops of water were added to a solution of (Bu$^t_2$bpy)$PdCl_2$ (445 mg, 1.00 mmol) in CH_2Cl_2 (60 mL). The reaction mixture was stirred for 6 h and then filtered. The filtrate was concentrate *in vacuo* to *ca.* 10 mL. Ether (30 mL) was added and the mixture was cooled at −30 °C for 3 h. The resulting fine microcrystalline pale yellow product was isolated by filtration. Yield: 365 mg (76%). The product was recrystallized from CH_2Cl_2–ether. Anal. calcd (found) for $C_{36}H_{50}N_4B_2F_8O_2Pd_2$: C, 45.17 (44.98); H. 5.26 (5.36); N, 5.85 (5.75%). ^{1}H NMR (300 MHz, CD_2Cl_2): 8.31 (d, J_{HH} = 6.0 Hz, 4H, 6,6′-H-bpy), 7.89 (d, J_{HH} = 1.6 Hz, 4H, 3,3′-H-bpy), 7.65 (dd, J_{HH} = 6.0 & 1.6 Hz, 4H, 5,5′-H-bpy), 1.43 (s, 36H, Bu^t), 0.28 (s, 2H, OH).

[Pt$_2$(μ-OH)(μ-O)(Bian)$_2$](BF$_4$) (1)

Method A. To a red solution of [Pt(μ-OH)(Bian)]$_2$(BF$_4$)$_2$ (50 mg, 0.031 mmol) dissolved in 3 mL of reagent grade CH_2Cl_2 was added ~10 equivalents of 1,8-bis(dimethylamino)-naphthalene. The reaction mixture was stirred for 15 min during which time it turned from red to purple. The mixture was stirred for an additional 15 min, passed through a pad of diatomaceous earth, and the volatiles removed *in vacuo* to give a purple solid. The solid was dissolved in a minimum volume of CH_2Cl_2 and ether was added to give a purple precipitate of the product contaminated with protonated 1,8-bis(dimethylamino)naphthalene salt which could not be eliminated.

Method B. To a red solution of [Pt(μ-OH)(Bian)]$_2$(BF$_4$)$_2$ (25 mg, 0.016 mmol) in 3 mL of reagent grade CH_2Cl_2 was added 4 mg of a crushed KOH pellet. The reaction mixture slowly turns purple after stirring for 15 min. At this point the stirring was stopped and the volatiles removed *in vacuo* to obtain a purple solid. The purple solid was dissolved in CH_2Cl_2, the solution passed through a pad of diatomaceous earth and the solvent evaporated to dryness to give the purple product in quantitative yield. ^{1}H NMR (CD_2Cl_2): 8.31 and 8.23 (overlapping d's, J_{HH} = 7.8 Hz, 2H and 2H, H_5 and $H_{5'}$), 7.50 (br t, J_{HH} ~ 8 Hz, 4H, H_4 and $H_{4'}$), 7.22–7.35 (m, 12H, $H_{10,11,12,10'11'12'}$), 6.93 (br d, J_{HH} ~ 7 Hz, 2H, H_3 or $H_{3'}$), 6.75 (br d, J_{HH} ~ 7 Hz, 2H, H_3 or $H_{3'}$), 3.30 (br sept, J_{HH} ~ 7 Hz, 4H, C*H*(CH$_3$)$_2$), 3.17 (br sept, J_{HH} ~ 7 Hz, 4H, C*H*(CH$_3$)$_2$), 1.33 (br d, J_{HH} ~ 7 Hz, 12H, CH(C*H*$_3$)$_2$), 1.12 (br d, J_{HH} ~ 7 Hz, 12H, CH(C*H*$_3$)$_2$), 0.96 (br d, J_{HH} ~ 7 Hz, 12H, CH(C*H*$_3$)$_2$), 0.90 (br d, J_{HH} ~ 7 Hz, 12H, CH(C*H*$_3$)$_2$), −1.84 (br s, 1H, OH). The ^{1}H NMR spectrum is often broadened due to trace protic impurities but sharpens on addition of 1,8-bis(dimethylamino)naphthalene. Crystals were grown at room temperature by layering a CD_2Cl_2 solution with Et_2O. Crystal data: a = 18.4678(18) Å, b = 15.3307(15) Å, c = 24.099(2) Å, β = 99.058(2)°, monoclinic, $P2_1/c$.

[(Bu$^t_2$bpy)$_2$M$_2$(μ-OH)(μ-O)]BF$_4$. M = Pd

A solution of [{(Bu$^t_2$bpy)Pd(μ-OH)}]$_2$(BF$_4$)$_2$ (191 mg, 0.200 mmol) in CH_2Cl_2 (20 mL) was vigorously stirred with solid NaH (19.2 mg, 0.800 mmol). The mixture became yellow within 20 min. The mixture was further stirred for 20 h and then filtered. The filtrate was concentrated *in vacuo* to *ca.* 10 mL. Ether (20 mL) was added and the mixture was stored at −30 °C for 3 h. The resulting fine microcrystalline yellow product was isolated by filtration. Yield: 113 mg (72%). Anal. calcd (found) for $C_{36}H_{49}BF_4N_4O_2Pd_2{\cdot}0.5CH_2Cl_2$: C, 48.02 (47.60); H. 5.48 (5.61); N, 6.14 (6.01%). The product was recrystallized from CH_2Cl_2–ether. ^{1}H NMR (250 MHz, CD_2Cl_2): 8.66 (d, J_{HH} = 5.9 Hz, 4H, 6,6′-H-bpy), 7.95 (d, J_{HH} = 1.8 Hz, 4H, 3,3′-H-bpy), 7.73 (dd, J_{HH} = 5.9 and 1.8 Hz, 4H, 5,5′-H-bpy), 1.42 (s, 36H, Bu^t).

M = Pt (2)

Method A. A solution of [{(Bu$^t_2$bpy)Pt(μ-OH)}]$_2$(BF$_4$)$_2$ (227 mg, 0.200 mmol) in CH_2Cl_2 (20 mL) was vigorously stirred with solid NaH (19.2 mg, 0.800 mmol). The mixture changed from yellow to orange to red over a 30 min period. Stirring was continued for 6 h and then the mixture was filtered. The filtrate was concentrated *in vacuo* to *ca.* 10 mL. Ether (20 mL) was added and the mixture was stored at −30 °C for 24 h. The resulting brick red microcrystalline solid was isolated by filtration and dried *in vacuo*. Yield: 187 mg (89%).

Method B. A THF solution (2 mL) of 1,8-bis(dimethyl-amino)naphthalene (42.8 mg, 0.200 mmol) was added to a suspension of [(Bu$^t_2$bpy)Pt(μ-OH)]$_2$(BF$_4$)$_2$ (113 mg, 0.100 mmol) in THF (10 mL). The solution changed from yellow to orange within 10 min then after 30 min it became red. The reaction mixture was stirred for 16 h and then filtered. The resulting product was collected by filtration. Yield: 90.0 mg (86%). The product was recrystallized from CH_2Cl_2–ether. Anal. calcd (found) for $C_{36}H_{49}N_4BF_4O_2Pt_2{\cdot}0.7CH_2Cl_2$: C, 39.85 (38.82); H. 4.59 (4.61); N, 5.06 (4.96%). ^{1}H NMR (250 MHz, CD_2Cl_2): 9.33 (br s, 4H, 6,6′-H-bpy), 7.64 (d, J_{HH} = 2 Hz, 4H, 3,3′-H-bpy), 7.49 (dd, 6 and 2 Hz, 4H, 5,5′-H-bpy), 1.27 (s, 36H, Bu^t). The OH signal was not observed. UV-Vis (λ_{max}/nm, CH_2Cl_2): 380, 320, 305, 270, 250.

[(Bu$^t_2$bpy)$_2$Pt$_2$(μ-OH)(μ-OCH$_3$)](BF$_4$)(OTf) (3)

A solution of MeOTf (33.0 mg. 0.200 mmol) was added drop-wise to a stirred solution of [(Bu$^t_2$bpy)$_2$Pt$_2$(μ-OH)(μ-O)](BF$_4$) (20 mg, 0.019 mmol) in CH_2Cl_2 (10 mL). The mixture changed from red to yellow within 10 min. Stirring was continued for 2 h then the mixture was filtered. The filtrate was concentrate *in vacuo* to *ca.* 4 mL. Ether (12 mL) was added and mixture cooled at −30 °C for 24 h. The resulting yellow solid was isolated by filtration. Yield: 19.7 mg (90%). The product was recrystallized from CH_2Cl_2–ether. Anal. calcd (found) for $C_{38}H_{52}BF_7N_4O_5Pt_2S{\cdot}0.5(CH_2Cl_2)$: C, 36.89 (37.09); H, 4.26 (3.99); N, 4.47 (4.28%). ^{1}H NMR (250 MHz, CD_2Cl_2): 8.72 (d, J_{HH} = 6.1 Hz, 2H, 6-H-bpy), 8.68 (d, J_{HH} = 5.6 Hz, 2H, 6′-H-bpy), 7.93 (d, J_{HH} = 1.8 Hz, 2H, 3-H-bpy), 7.85 (d, J_{HH} = 1.8 Hz, 2H, 3′-H-bpy), 7.69 (dd, J_{HH} = 6.1 and 1.8 Hz, 2H, 5-H-bpy), 7.62 (dd, J_{HH} = 6.1 and 1.8 Hz, 2H, 5′-H-bpy), 4.21 (s, 1H, OH), 3.12 (s, 3H, Me), 1.44 (s, 18H, Bu^t), 1.42 (s, 18H, Bu^t).

[Pt(μ-O)(Bian)]$_2$ (4)

To a red solution of [Pt(μ-OH)(Bian)]$_2$(BF$_4$)$_2$ (50 mg, 0.031 mmol) dissolved in 3 mL of CH_2Cl_2 was added a 10 mg portion of a

crushed KOH pellet and one drop of water. The reaction mixture turned purple after stirring for 15 min, and then finally became the dark blue of the product after two hours of stirring. The reaction mixture was then evaporated to dryness, the residue dissolved in a minimum amount of CH_2Cl_2, passed through a pad of diatomaceous earth, and the volatiles removed *in vacuo*. The resulting blue solid product was washed with petroleum ether and dried *in vacuo*. Yield (35 mg, 80%). ^{1}H NMR (CD_2Cl_2): 8.10 (d, $J_{HH} = 8.2$ Hz, 4H, H_5), 7.39 (t, $J_{HH} = 7.7$ Hz, 4H, H_{11}), 7.24 (d, $J_{HH} = 7.7$ Hz, $H_{10,12}$), 7.12 (t, $J_{HH} = 7.7$ Hz, 4H, H_4), 6.55 (d, $J_{HH} = 7.1$ Hz, 4H, H_3), 3.38 (sept, $J_{HH} = 6.9$ Hz, 8H, $CH(CH_3)_2$), 1.22 (d, $J_{HH} = 6.9$ Hz, 24H, $CH(CH_3)_2$), 0.82 (d, $J_{HH} = 6.9$ Hz, 24H, $CH(CH_3)_2$). Anal. calcd (Found) for $C_{72}H_{80}N_4O_2Pt_2 \cdot 0.5\ CH_2Cl_2$: C, 59.44 (59.40); H, 5.58 (5.57); N, 3.73 (3.83%).

[(Bian)$_2$Pt$_2$(μ$_2$-O)(μ$_3$-OAuPPh$_3$)](BF$_4$) (5)

To a solution of **4** (15 mg, 0.011 mmol) dissolved in 2 mL of CH_2Cl_2 was added 10 mg of freshly prepared "Ph_3PAuBF_4" (from Ph_3PAuCl and $AgBF_4$ in THF)[93] in CH_2Cl_2. The reaction mixture changed from blue to dark purple. The reaction mixture was stirred for 20 min and then the volatiles were removed *in vacuo*. The residue was washed with petroleum ether and dried *in vacuo* to give the bluish-purple solid product. Yield (25 mg, 91%). Crystals suitable for X-ray diffraction and analysis were grown at room temperature by layering a CH_2Cl_2 solution with toluene. Anal. calcd (Found) for $C_{90}H_{95}AuBF_4N_4O_2PPt_2$: C, 54.88 (55.14); H, 4.86 (4.73); N, 2.85 (2.76%). ^{1}H NMR (CD_2Cl_2, −20 °C): 8.24 (d, $J_{HH} = 8.2$ Hz, 4H, H_5), 7.50–7.18 (m, 31H, PPh_3 and $H_{4,10,11,12}$), 6.76 (d, $J_{HH} = 7.2$ Hz, 4H, H_3), 3.55 (br sept, $J_{HH} = 6.5$ Hz, 4H, $CH(CH_3)_2$), 3.10 (br sept, $J_{HH} = 6.6$ Hz, 4H, $CH(CH_3)_2$), 1.07 (d, $J_{HH} = 6.6$ Hz, 12H, $CH(CH_3)_2$), 0.98 (d, $J_{HH} = 6.6$ Hz, 12H, $CH(CH_3)_2$), 0.72 and 0.70 (overlapping d's, $J_{HH} = 6.6$ Hz, 12H and 12H, $CH(CH_3)_2$). ^{31}P NMR (CH_2Cl_2, 101 MHz, −20 °C): 22.9 (s). Spectra (the 2,6-$Pr^i_2C_6H_3$ signals only) are broadened at 25 °C due to exchange with traces of Ph_3PAuCl, which is visible at 32 ppm in the ^{31}P NMR spectrum. Identical NMR spectra are observed with mixtures of **4** and Ph_3PAuCl.

[(Bian)$_2$Pt$_2$(μ-O)(μ-OMe)]OTf (6)

To a stirred solution of **4** (15 mg, 0.011 mmol) dissolved in 4 mL of toluene was added methyl triflate (3 mg, 0.02 mmol) in 1 mL of toluene. A purple solid precipitated from the mixture. The dark purple solid was isolated by filtration, washed with pentane and dried *in vacuo*. Yield (11 mg, 75%). Crystals for the X-ray analysis were obtained by layering a CH_2Cl_2 solution with toluene. Anal. calcd. (Found) for $C_{74}H_{83}F_3N_4O_5Pt_2S$: C, 55.97 (55.64); H, 5.27 (5.54); N, 3.53 (3.93%). ^{1}H NMR (CD_2Cl_2, 25 °C): 8.29 and 8.26 (overlapping d's, $J_{HH} = 8$ Hz, 2H and 2H, $H_{5,5'}$), 7.52 (t, $J_{HH} = 7.5$ Hz, 4H, $H_{4,4'}$) 7.40–7.28 (m, 8H, $H_{11,11'}$ and $H_{10,10'}$ or $H_{12,12'}$), 7.22 (d, $J_{HH} = 7.5$ Hz, 4H, $H_{10,10'}$ or $H_{12,12'}$), 6.70 (d, $J_{HH} = 7.2$ Hz, 4H, H_3 or $H_{3'}$) 6.59 (d, $J_{HH} = 7.2$ Hz, 4H, H_3 or $H_{3'}$), 3.38 (sept, $J_{HH} = 6.8$ Hz, 4H, $CH(CH_3)_2$), 3.12 (septet, $J_{HH} = 6.8$ Hz, 4H, $CH(CH_3)_2$), 2.48 (s with broad base, 3H, OMe), 1.40 (d, $J_{HH} = 6.8$ Hz, 12H, $CH(CH_3)_2$), 1.13 (d, $J_{HH} = 6.8$ Hz, 12H, $CH(CH_3)_2$), 0.92 (d, $J_{HH} = 6.8$ Hz, 12H, $CH(CH_3)_2$), 0.85 (d, $J_{HH} = 6.8$ Hz, 12H, $CH(CH_3)_2$). ^{19}F NMR (CD_2Cl_2, 25 °C): −79.0. Crystals were grown at room temperature by layering a CD_2Cl_2 solution with toluene. Crystal data: $a = 16.346(3)$ Å, $b = 28.541(6)$ Å, $c = 15.987(3)$ Å, $\beta = 99.362(4)°$, monoclinic, $P2_1/c$.

Reaction of [Pt(μ-O)(Bian)]$_2$ (4) with excess MeOTf

To a solution of **4** (10 mg, 0.0070 mmol) dissolved in 4 mL of CH_2Cl_2 was added methyl triflate (6.0 mg, 0.036 mmol) in 2 mL of CH_2Cl_2. As the mixture was stirred over an hour the color changed from blue to purple and later to dark-red. The dark-red solution was evaporated to dryness, washed with pentane and dried *in vacuo* to give an incompletely characterized red compound that may be [(Bian)Pt(OTf)$_2$]. Yield (8.0 mg, 85%). ^{1}H NMR (CD_2Cl_2, 25 °C): 8.29 (d, $J_{HH} = 7.5$ Hz, 4H, H_5), 7.33 (d, $J_{HH} = 7.5$ Hz, 8H, H_{10}), 7.60–7.51 (overlapping t, $J_{HH} = 7.5$ Hz, 8H, H_4 and H_{11}) 6.78 (d, $J_{HH} = 7.5$ Hz, 4H, H_3), 3.41 (septet, $J_{HH} = 7.5$ Hz, 8H, $CH(CH_3)_2$), 1.21 (d, $J_{HH} = 7.5$ Hz, 24H, $CH(CH_3)_2$), 0.82 (d, $J_{HH} = 7.5$ Hz, 24H, $CH(CH_3)_2$. ^{19}F NMR (CD_2Cl_2, 25 °C): −79.04.

Reaction of [Pt(μ-O)(Bian)]$_2$ (4) with [Pt(COD)(OTf)$_2$]: [(Bian)(COD)$_2$Pt$_3$(μ-OH)$_3$](OTf)$_3$ (7)

[Pt(COD)(OTf)$_2$] (9.0 mg, 0.015 mmol) in 1 mL of CH_2Cl_2 was added drop-wise to a blue solution of **4** (10 mg, 0.0070 mmol) dissolved in 4 mL of CH_2Cl_2. The reaction slowly changed from blue to purple and finally to yellow brown. The dark-yellow brown solution was concentrated, layered with ether, and stored at −30 °C to give a brown solid. ^{1}H NMR of the brown solid (CD_2Cl_2): 8.33 (d, $J_{HH} = 7.5$ Hz, H_5), 7.60–7.51 (overlapping t, $J_{HH} = 7.5$ Hz, H_4 and H_{11}), 7.33 (d, $J_{HH} = 7.5$ Hz, H_{10}), 6.79 (d, $J_{HH} = 7.5$ Hz, H_3), 5.67 (br s with satellites, $J_{Pt-H} = 68$ Hz, COD), 3.25 (sept, $J_{HH} = 6.7$ Hz, $CH(CH_3)_2$), 2.76 (br m, COD), 2.23 (br d, $J_{Pt-H} = 8$ Hz, COD), 1.37 (d, $J_{HH} = 6.7$ Hz, $CH(CH_3)_2$), 0.83 (d, $J_{HH} = 6.7$ Hz, 24H, $CH(CH_3)_2$). The Bian to COD ratio was ~1 : 1 by integration. A few orange-red crystals deposited from a CH_2Cl_2 solution of the brown solid over a 4-day period at room temperature. The orange-red crystals were characterized by X-ray diffraction as the trihydroxo complex [(Bian)(COD)$_2$Pt$_3$(μ-OH)$_3$](OTf)$_3$ (**7**).

[(Bu$^t_2$bpy)$_3$Ni$_3$(μ$_3$-O)$_2$](BF$_4$)$_2$ (8)

A solution of Ni(Bu^{t}bpy)Cl$_2$ (30 mg, 0.075 mmol) in CH_2Cl_2 (3 mL) was added to a stirred solution of [(LAu)$_3$(μ$_3$-O)]BF$_4$ (74 mg, 0.050 mmol) in CH_2Cl_2 (3 mL). The mixture changed from yellow to red within 5 min. The reaction was further stirred for 25 min and then concentrated *in vacuo* to *ca.* 3 mL. THF (6 mL) was added and the mixture was cooled at −30 °C for 24 h. The resulting fine microcrystalline red product was isolated by filtration. Yield: 66 mg (74%). Crystals for the X-ray analysis were obtained by slow recrystallization from CH_2Cl_2–THF. Anal. calcd (found) for $C_{54}H_{72}N_6Ni_3O_2B_2F_8$: C, 54.65 (53.00); H. 6.11 (5.43); N, 7.08 (6.37%). ^{1}H NMR (250 MHz, CD_2Cl_2): 8.11 (d, $J_{HH} = 5.9$ Hz, 6H, 6,6′-H-bpy), 7.84 (d, $J_{HH} = 1.8$ Hz, 6H, 3,3′-H-bpy), 7.66 (dd, $J_{HH} = 5.9$ and 1.8 Hz, 6H, 5,5′-H-bpy), 1.40 (s, 54H, Bu^t).

[(Bu$^t_2$bpy)Pt(μ$_3$-O)(AuPPh$_3$)]$_2$(BF$_4$)$_2$ (9, M = Pt)

A solution of Pt(Bu$^t_2$bpy)Cl$_2$ (106 mg, 0.200 mmol) in CH_2Cl_2 (3 mL) was added to a stirred solution of [(LAu)$_3$(μ$_3$-O)]BF$_4$ (296 mg. 0.200 mmol) in CH_2Cl_2 (3 mL). The mixture changed

from yellow to golden-yellow within 15 min. The reaction was further stirred for 25 min and then concentrated *in vacuo* to *ca.* 3 mL. Toluene (6 mL) was added and the mixture was stored at −30 °C for 24 h. The resulting fine microcrystalline yellow-orange product was isolated by filtration. Yield: 150 mg (73%). Crystals for X-ray analysis were obtained by recrystallization from CD_2Cl_2–ether. Anal. calcd (found) for $C_{72}H_{78}N_4Au_2B_2F_8O_2P_2Pt_2$: C, 42.14 (42.13); H. 3.80 (3.87); N, 2.73 (2.80%). ^{1}H NMR (300 MHz, CD_2Cl_2): 9.00 (d, 4H, J_{HH} = 6.0 Hz, 6,6′-H-bpy), 8.09 (d, 4H, J_{HH} = 1.8 Hz, 3,3′-H-bpy), 7.58 (dd, 4H, J_{HH} = 6.1 Hz, J_{HH} = 1.9 Hz, 5,5′-H-bpy), 7.44–7.24 (m, 30 H, Ph), 1.45 (s, 36H, Bu^t). ^{31}P{^{1}H} NMR (101 MHz, CD_2Cl_2): 23.1 (s). ^{195}Pt NMR (64 MHz, CD_2Cl_2): −1255 (s).

[(Bu$^t_2$bpy)$_2$Pt$_2$(μ-OH)(μ-NHAr)](BF$_4$)$_2$ (11). Ar = 4-tol

A CH_2Cl_2 solution (5 mL) of *p*-toluidine (75.3 mg, 0.704 mmol) was added to a stirred solution of [(Bu$^t_2$bpy)Pt(μ-OH)]$_2$(BF$_4$)$_2$ (200 mg, 0.176 mmol) in CH_2Cl_2 (50 mL). The mixture changed from yellow to orange within 20 min. The reaction was further stirred for 2 h and then filtered. The filtrate was concentrated *in vacuo* (15 mL). To this solution ether (30 mL) was added and the apricot colored product was isolated by filtration. Yield: 200 mg (93%). The product was recrystallized from CH_2Cl_2–ether. Anal. calcd (found) for $C_{43}H_{57}N_5B_2F_8OPt_2$: C, 42.19 (42.27); H. 4.66 (4.79); N, 5.72 (5.58%).

MS (ESI/APC-direct infusion, CH_2Cl_2, *m*/*z*): 1136.4 (10%, [{($C_{18}H_{24}N_2$)$_2$Pt$_2$(μ-OH)(μ-NHC$_6$H$_4$CH$_3$-4)}]$^+$), 1048.4 (13%, [{($C_{18}H_{24}N_2$)$_2$Pt$_2$(μ-OH)(μ-NHC$_6$H$_4$CH$_3$-4)}]$^{2+}$), 525.1 (23%, [($C_{18}H_{24}N_2$)Pt(C_7H_8N)(OH)/2]), 516.0 (100%, [($C_{18}H_{24}N_2$)Pt(C_7H_8N)/2]). ^{1}H NMR (300 MHz, CD_2Cl_2): 8.78 (d, 2H, J_{HH} = 5.6 Hz, 6-H-bpy), 8.40 (d, 2H, J_{HH} = 5.9 Hz, 6′-H-bpy), 8.14 (d, 2H, J_{HH} = 8.3 Hz, 2,2′-H-*p*-tol), 7.86 (s, 2H, 3-H-bpy), 7.81 (s, 2H, 3′-H-bpy), 7.78 (d, 2H, J_{HH} = 4.6 Hz, 5-H-bpy), 7.57 (d, 2H, J_{HH} = 5.3 Hz, 5′-H-bpy), 7.19 (d, 2H, J_{HH} = 8.2 Hz, 3,3′-H-*p*-tol), 5.17 (s, 1H, NH), 2.55 (s, 1H, OH), 2.25 (s, 3H, Me-*p*-tol), 1.44 (s, 18H, Bu^t), 1.39 (s, 18H, Bu^t).

Ar = Ph

Method A. A solution of [(Bu$^t_2$bpy)Pt(μ-OH)]$_2$(BF$_4$)$_2$ (283.5 mg, 0.250 mmol) in CH_2Cl_2 (25 mL) was added to a stirred solution of aniline (93.0 mg, 1.00 mmol) in CH_2Cl_2 (5 mL). The mixture changed from yellow to red within 20 min. The reaction was further stirred for 4 h and then filtered. The filtrate was concentrate *in vacuo* to *ca.* 10 mL. Ether (20 mL) was added and the resulting fine microcrystalline yellow-orange product was isolated by filtration. Yield: 245 mg (81%).

Method B. A solution of LiPhNH (99.0 mg, 1.00 mmol) in CH_2Cl_2 (5 mL) was added to a stirred solution of [(Bu$^t_2$bpy)Pt(μ-OH)]$_2$(BF$_4$)$_2$ (283.5 mg, 0.250 mmol) in CH_2Cl_2 (20 mL). Within 30 min the color of the mixture changed from yellow to red. The mixture was further stirred for 4 h and then filtered. The filtrate was concentrate *in vacuo* to *ca.* 10 mL. Ether (20 mL) was added and the resulting fine microcrystalline yellow-orange product was isolated by filtration. Yield: 240 mg (79%). Anal. calcd (found) for $C_{42}H_{55}N_5B_2F_8OPt_2\cdot1.5CH_2Cl_2$: C, 39.08 (39.11); H. 4.37 (4.48); N, 5.24 (5.04%). ^{1}H NMR (300 MHz, CD_2Cl_2): 8.78 (d, J_{HH} = 6.0 Hz, 2H, 6-H-bpy), 8.41 (d, J_{HH} = 6.3 Hz, 2H, 6′-H-bpy), 8.26 (d, J_{HH} = 7.8 Hz, 2H, 2,2′-H-aniline), 7.88 (d, J_{HH} = 1.5 Hz, 2H, 3-H-bpy), 7.82 (d, J_{HH} = 1.8 Hz, 2H, 3′-H-bpy), 7.78 (dd, J_{HH} = 6.0 and 1.5 Hz, 2H, 5-H-bpy), 7.57 (dd, J_{HH} = 6.3 and 2.1 Hz, 2H, 5′-H-bpy), 7.39 (t, J_{HH} = 7.6 Hz, 1H, 3-H-aniline), 7.15 (t, J_{HH} = 6.6, 1H, 3′-H-aniline), 5.20 (s, 1H, NH), 2.55 (br s, 1H, OH), 1.44 (s, 18H, Bu^t), 1.38 (s, 18H, Bu^t).

Ar = 4-C$_6$H$_4$NO$_2$

A solution of 4-nitroaniline (97.0 mg, 0.704 mmol) was added to a stirred solution of [(Bu$^t_2$bpy)Pt(μ-OH)]$_2$(BF$_4$)$_2$ (200 mg, 0.176 mmol) in CH_2Cl_2 (50 mL). The solution turned from yellow to orange within 20 min. The reaction was further stirred for 24 h and then filtered. The resulting filtrate was concentrated *in vacuo* to *ca.* 15 mL. To this solution ether (30 mL) was added and the product was isolated by filtration. Yield: 326 mg (74%). Crystals for an X-ray analysis were obtained by recrystallization from CD_2Cl_2–ether at −30 °C but these gave very poor results and contained badly disordered solvent molecules. ^{1}H NMR (300 MHz, CD_2Cl_2): 8.75 (d, 2H, J_{HH} = 5.8 Hz, 6-H-bpy), 8.46 (d, 2H, J_{HH} = 8.9 Hz, 2,2′-H-*p*-nitroaniline), 8.41 (d, 2H, J_{HH} = 6.2 Hz, 6′-H-bpy), 8.23 (d, 2H, J_{HH} = 8.9 Hz, 3,3′-H-*p*-nitroaniline), 7.87 (d, 2H, 3-H-bpy), 7.83 (d, 2H, J_{HH} = 1.4 Hz, 3′-H-bpy), 7.79 (d, 2H, J_{HH} = 6.0, 5-H-bpy), 7.60 (d, 2H, J_{HH} = 4.3, 5′-H-bpy), 5.66 (s, 1H, NH), 2.83 (s, 1H, OH), 1.45 (s, 18H, Bu^t), 1.39 (s, 18H, Bu^t).

[(Bu$^t_2$bpy)Pd(μ-NHAr)]$_2$(BF$_4$)$_2$ (12). Ar = Ph

Method A. A solution of aniline (93.0 mg, 1.00 mmol) in CH_2Cl_2 (5 mL) was added to [(Bu$^t_2$bpy)Pd(μ-OH)]$_2$(BF$_4$)$_2$ (239 mg, 0.250 mmol) in CH_2Cl_2 (50 mL). The mixture changed from yellow to red within 30 min. The reaction was stirred for 4 h and then filtered. The filtrate was concentrate *in vacuo* to *ca.* 15 mL. To this solution ether (30 mL) was added and the resulting fine microcrystalline yellow product was isolated by filtration. Yield: 221 mg (80%).

Method B. A CH_2Cl_2 solution (5 mL) of LiPhNH (99.0 mg, 1.00 mmol) was added to a stirred solution of [(Bu$^t_2$bpy)Pd(μ-OH)]$_2$(BF$_4$)$_2$ (239 mg, 0.250 mmol) in CH_2Cl_2 (50 mL). Within 30 min the color of reaction changed from yellow to red. The reaction was further stirred for 4 h and then filtered. The filtrate was concentrate *in vacuo* to *ca.* 15 mL. Ether (30 mL) was added and the resulting fine microcrystalline yellow product was isolated by filtration. Yield: 219 mg (79%). Crystals for the X-ray analysis were obtained by recrystallization from THF–ether at −30 °C. Anal. calcd (found) for $C_{48}H_{60}B_2F_8N_6Pd_2\cdot0.5(CH_2Cl_2)$: C, 50.66 (50.43); H. 5.35 (5.26); N, 7.31 (6.93%). ^{1}H NMR (250 MHz, CD_2Cl_2): 8.59 (d, J_{HH} = 7.5 Hz, 4H, NC$_6$H$_5$), 8.17 (d, J_{HH} = 6.2 Hz, 4H, 6,6′-H-bpy), 7.79 (d, J_{HH} = 1.8 Hz, 4H, 3,3′-H-bpy), 7.55 (dd, J_{HH} = 6.2 and 1.8 Hz, 4H, 5,5′-H-bpy), 7.31 (t, J_{HH} = 8.8 Hz, 4H, NC$_6$H$_5$), 7.03 (t, J_{HH} = 7.5 Hz, 2H, NC$_6$H$_5$), 2.89 (s, 2H, NH), 1.35 (s, 36H, Bu^t).

Ar = 4-tol

A solution of [(Bu$^t_2$bpy)Pd(μ-OH)]$_2$(BF$_4$)$_2$ (239 mg, 0.250 mmol) in CH_2Cl_2 (50 mL) was reflux with *p*-toluidine (107 mg, 1.00 mmol) with stirring for 20 h and then filtered. The filtrate was concentrate

in vacuo to *ca.* 15 mL. Ether (30 mL) was added and the resulting fine microcrystalline yellow product was isolated by filtration. Yield: 230 mg (81%). Crystals for the X-ray analysis were obtained by recrystallization from CD_2Cl_2–ether at −30 °C. Anal. calcd (found) for $C_{50}H_{64}N_6B_2F_8Pd_2$: C, 52.86 (52.05); H. 5.63 (5.65); N, 7.40 (7.20%). (The low carbon value probably results from occluded CH_2Cl_2.) ^{1}H NMR (300 MHz, CD_2Cl_2): 8.52 (d, J_{HH} = 8.2 Hz, 4H, H-*p*-tol), 8.26 (d, J_{HH} = 6.0 Hz, 4H, 6,6′-H-bpy), 7.68 (d, J_{HH} = 1.8 Hz, 4H, 3,3′-H-bpy), 7.55 (dd, J_{HH} = 6.0 & 1.8 Hz, 4H, 5,5′-H-bpy), 7.09 (d, J_{HH} = 8.2 Hz, 4H, H-*p*-tol), 2.83 (s, 2H, NH), 2.17 (s, 6H, Me-*p*-tol), 1.34 (s, 36H, Bu^t).

Ar = 4-$C_6H_4NO_2$

A solution of $[(Bu^t_2bpy)Pd(\mu\text{-}OH)]_2(BF_4)_2$ (150 mg, 0.157 mmol) in CH_2Cl_2 (50 mL) was refluxed with 4-nitroaniline (87.0 mg, 0.630 mmol). The bright yellow solution was further refluxed with stirring for 5 h and then filtered. The filtrate was concentrate *in vacuo* to *ca.* 15 mL. Ether (30 mL) was added and the resulting fine microcrystalline yellow product was isolated by filtration. Yield: 172 mg (91%). The product was recrystallized from CH_2Cl_2–ether. Anal. calcd (found) for $C_{48}H_{58}N_8O_4B_2F_8Pd_2$: C, 48.16 (48.34); H. 4.84 (4.31); N, 9.36 (9.10%). ^{1}H NMR (300 MHz, CD_2Cl_2): 8.79 (d, J_{HH} = 8.8 Hz, 4H, H-*p*-nitroaniline), 8.19 (d, J_{HH} = 8.8 Hz, 4H, H-*p*-nitroaniline), 8.14 (d, J_{HH} = 6.0 Hz, 4H, 6,6′-H-bpy), 7.81 (d, J_{HH} = 1.9 Hz, 4H, 3,3′-H-bpy), 7.59 (dd, J_{HH} = 6.0, 4H, 1.9 Hz, 5,5′-H-bpy), 3.54 (s, 2H, NH), 1.36 (s, 36H, Bu^t).

$[(Bu^t_2bpy)Pt(\mu\text{-}NH\text{-}4\text{-}tol)]_2(BF_4)_2$ (13)

A solution of *p*-toluidine (42.8 mg, 0.400 mmol) was added to a suspension of $[(Bu^t_2bpy)_2Pt_2(\mu\text{-}OH)(\mu\text{-}NH\text{-}4\text{-}tol)](BF_4)_2$ (245 mg, 0.200 mmol) in CH_2Cl_2 (50 mL). The solution was stirred for 20 h and then filtered. The filtrate was concentrate *in vacuo* to *ca.* 15 mL. To this solution ether (30 mL) was added and the amber product was isolated by filtration. Yield: 210 mg (80%). The product was recrystallized from CD_2Cl_2–ether. Anal. calcd (found) for $C_{50}H_{64}N_6B_2F_8Pt_2$: C, 45.73 (45.14); H. 4.87 (4.99); N, 6.40 (6.27%). ^{1}H NMR (300 MHz, CD_2Cl_2): 8.47 (d, 4H, J_{HH} = 6.1 Hz, 6,6′-H-bpy), 8.31 (d, 4H, J_{HH} = 8.2 Hz, 2,2′-H-*p*-tol), 7.81 (d, 4H, J_{HH} = 1.9 Hz, 3,3′-H-bpy), 7.61 (dd, 4H, J_{HH} = 6.2 and 2.0 Hz, 5,5′-H-bpy), 7.16 (d, 4H, J_{HH} = 8.1 Hz, 3,3′-H-*p*-tol), 4.97 (s, 2H, NH), 2.25 (s, 6H, Me-*p*-tol), 1.40 (s, 36H, Bu^t).

$[(Bu^t_2bpy)_2Pt_2(\mu\text{-}NH\text{-}4\text{-}tol)(\mu\text{-}O)]BF_4$ (14)

Method A. A solution of $[(Bu^t_2bpy)_2Pt_2(\mu\text{-}OH)(\mu\text{-}NH\text{-}4\text{-}tol)](BF_4)_2$ (122 mg, 0.100 mmol) in THF (50 mL) was vigorously stirred with solid NaH (4.80 mg, 0.200 mmol). The solution became orange within 30 min. Stirring was continued for 3 h and then the mixture was filtered. The filtrate was reduced *in vacuo* to *ca.* 15 mL. To this solution ether (30 mL) was added and the resulting orange solid product was isolated by filtration. Yield: 98.0 mg (87%).

Method B. A THF solution (5 mL) of *p*-toluidine (94.1 mg, 0.880 mmol) was added to a suspension of $[(Bu^t_2bpy)Pt(\mu\text{-}OH)]_2(BF_4)_2$ (249 mg, 0.220 mmol) in THF (50 mL). The reaction mixture was brought to reflux with stirring. Over 6 h the solution became deep yellow and an orange solid deposited. The orange solid was collected by filtration. Yield: 113.0 mg (45%).

Method C. A THF solution (2 mL) of proton sponge (68.5 mg, 0.320 mmol) was added to a stirred solution/suspension of $[(Bu^t_2bpy)_2Pt_2(\mu\text{-}OH)(\mu\text{-}NHC_6H_4Me\text{-}4)](BF_4)_2$ (195 mg, 0.160 mmol) in THF (30 mL). The reaction mixture was refluxed with stirring for 6 h. The resulting solid product was collected by filtration. Yield: 137.0 mg (75%). The product was recrystallized from CH_2Cl_2–ether. Anal. calcd (found) for $C_{43}H_{56}N_5BF_4OPt_2\cdot 0.5NaBF_4$ (method A): C, 43.37 (42.97); H. 4.74 (4.75); N, 5.88 (5.89%). MS (ESI/APC-direct infusion, CH_2Cl_2, *m*/*z*): 1084.4 (90%, $[(C_{18}H_{24}N_2)_2Pt_2(\mu\text{-}O)(\mu\text{-}NHC_6H_4CH_3\text{-}4)]^+$), 568.0 (100%, $[(C_{18}H_{24}N_2)Pt(\mu\text{-}NC_6H_4CH_3\text{-}4)]$), 268.9 (24%, $[C_{18}H_{24}N_2]$). ^{1}H NMR (300 MHz, CD_2Cl_2): 10.28 (d, 2H, 6-H-bpy), 8.14 (d, 2H, J_{HH} = 5.8 Hz, 2,2′-H-*p*-tol), 7.68 (d, 2H, J_{HH} = 4.4 Hz, 6′-H-bpy), 7.60 (d, 2H, 3-H-bpy), 7.55 (d, 2H, 5-H-bpy), 7.43 (d, 2H, 3′-H-bpy), 7.14 (d, 2H, 3,3′-H-*p*-tol), 5.46 (s, 1H, NH), 2.32 (s, 3H, Me-*p*-tol), 1.31 (s, 18H, Bu^t), 1.04 (s, 18H, Bu^t).

$[(Bu^t_2bpy)Pt(\mu\text{-}N\text{-}4\text{-}tol)]_2$ (15)

A solution of $[(Bu^t_2bpy)Pt(\mu\text{-}NH\text{-}4\text{-}tol)]_2(BF_4)_2$ (91.8 mg, 0.070 mmol) in CH_2Cl_2 (50 mL) was vigorously stirred with solid Bu^{t}OK (17.0 mg, 0.070 mmol). The solution color changed from yellow to black green within 10 min. Stirring was continued for 15 h and then the mixture was filtered. The volume of the filtrate was reduced *in vacuo* to *ca.* 15 mL. Ether (30 mL) was added and the resulting dark green product was isolated by filtration. Yield: 68.0 mg (74%). Anal. calcd (found) for $C_{50}H_{62}N_6Pt_2$: C, 52.81 (52.35); H. 5.50 (5.12); N, 7.39 (7.05%). ^{1}H NMR (300 MHz, CD_2Cl_2): 9.06 (d, 4H, J_{HH} = 6.1 Hz, 6,6′-H-bpy), 8.71 (d, 4H, J_{HH} = 8.0 Hz, 2,2′-H-*p*-tol), 7.73 (d, 4H, J_{HH} = 1.6 Hz, 3,3′-H-bpy), 7.61 (dd, 4H, J_{HH} = 6.0 AND Hz, 1.9-H-bpy), 7.07 (d, 4H, J_{HH} = 7.9 Hz, 3,3′-H-*p*-tol), 2.17 (s, 6H, Me-*p*-tol), 1.35 (s, 36H, Bu^t).

$(Bu^t_2bpy)Pd(OTf)_2$ (16). M = Pd

A solution of $Pd(Bu^t_2bpy)Cl_2$ (44.5 mg, 0.100 mmol) in CH_2Cl_2 (3 mL) was stirred with solid $AgSO_3CF_3$ (51.4 mg, 0.200 mmol) for 1 h in the absence of light. The reaction mixture changed from yellow to golden-yellow within 15 min with a pale purple precipitate of AgCl. The yellow solution was collected by filtration and then dried *in vacuo*. The solid was recrystallized from CH_2Cl_2–ether. Yield: 61.2 mg (91%). Crystals for X-ray analysis were obtained by recrystallization from CD_2Cl_2–ether. Anal. calcd (found) for $C_{20}H_{24}N_2PdS_2O_6F_8$: C, 35.71 (35.62); H. 3.57 (3.61); N, 4.16 (3.97%). ^{1}H NMR (250 MHz, CD_2Cl_2): 8.69 (d, 2H, J_{HH} = 6.3 Hz, 6,6′-H-bpy), 7.83 (d, 2H, J_{HH} = 2.0 Hz, 3,3′-H-bpy), 7.64 (dd, 2H, J_{HH} = 6.3 Hz, J_{HH} = 2.1 Hz, 5,5′-H-bpy), 1.44 (s, 18H, Bu^t).

M = Pt

This known complex[55] was prepared similarly to the Pd analog using $Pt(Bu^t_2bpy)Cl_2$ (53.4 mg, 0.100 mmol) in place of $Pd(Bu^t_2bpy)Cl_2$. Yield: 55.0 mg (90%). Anal. calcd (found) for $C_{20}H_{24}N_2PtS_2O_6F_8$: C, 31.53 (31.43); H. 3.15 (3.29); N, 3.67 (3.46%). ^{1}H NMR (300 MHz, CD_2Cl_2): 8.64 (d, 2H, J_{HH} = 6.3 Hz,

6,6′-H-bpy), 7.90 (d, 2H, $J_{HH} = 1.9$ Hz, 3,3′-H-bpy), 7.69 (dd, 2H, $J_{HH} = 6.3$ Hz, $J_{HH} = 2.1$ Hz, 5,5′-H-bpy), 1.45 (s, 18H, Bu^t). ^{195}Pt NMR (64 MHz, CD_2Cl_2): −3084.4 (s).

[(Bu$^t_2$bpy)Pt(OH$_2$)$_2$](OTf)$_2$ (17)

A solution of [(Bu$^t_2$bpy)Pt(OTf)$_2$] (20.0 mg, 0.025 mmol) in CH_2Cl_2 (6 mL) was stirred with 2 equiv of water. The reaction was further stirred for 2 h and then concentrated *in vacuo* to *ca.* 3 mL. Ether (6 mL) was added and the mixture was cooled at −30 °C for 24 h. The resulting fine microcrystalline yellow solid was isolated by filtration. Yield: 19.7 mg (94%). Crystals for the X-ray analysis were obtained from CD_2Cl_2–ether at −30 °C (ether solvate) or by slow evaporation (in the drybox) of a CH_2Cl_2 solution (unsolvated). Anal. calcd (found) for $C_{20}H_{28}N_2PtS_2O_8F_8$: C, 28.75 (28.19); H. 3.38 (3.21); N, 3.35 (3.10%). ^{1}H NMR (250 MHz, CD_2Cl_2): 8.56 (d, 2H, $J_{HH} = 6.2$ Hz, 6,6′-H-bpy), 8.27 (s, 4H, H_2O), 7.95 (d, 2H, $J_{HH} = 1.9$ Hz, 3,3′-H-bpy), 7.72 (dd, 2H, $J_{HH} = 6.3$ Hz, $J_{HH} = 2.1$ Hz, 5,5′-H-bpy), 1.47 (s, 18H, Bu^t).

Acknowledgements

Support from the Chemical Sciences, Geosciences and Biosciences Division, Office of Basic Energy Sciences, Office of Science, U. S. Department of Energy (DE-FG02-88ER13880) is gratefully acknowledged. A grant from the National Science Foundation (9221835) provided a portion of the funds for the purchase of the NMR equipment. We thank Chad Magee for initial synthetic work on **1** and Dr Charles Barns for X-ray data collection and processing.

References

1 J. R. Fulton, A. W. Holland, D. J. Fox and R. G. Bergman, *Acc. Chem. Res.*, 2002, **35**, 44.
2 R. G. Bergman, *Polyhedron*, 1995, **14**, 3227.
3 H. E. Bryndza and W. Tam, *Chem. Rev.*, 1988, **88**, 1163.
4 M. D. Fryzuk and C. D. Montgomery, *Coord. Chem. Rev.*, 1989, **95**, 1.
5 P. R. Sharp, *J. Chem. Soc., Dalton Trans.*, 2000, 2647.
6 S. J. Berners-Price and T. G. Appleton, in *Platinum-Based Drugs in Cancer Therapy*, ed. L. R. Kelland and N. P. Farrell, Humana Press, NJ, USA, 2000, p. 3.
7 S. E. Sherman and S. J. Lippard, *Chem. Rev.*, 1987, **87**, 1153.
8 L. Que, Jr. and W. B. Tolman, *Angew. Chem., Int. Ed.*, 2002, **41**, 1114.
9 A. G. Blackman and W. B. Tolman, *Struct. Bonding*, 2000, **97**, 179.
10 P. L. Holland and W. B. Tolman, *Coord. Chem. Rev.*, 1999, **192**, 855.
11 W. B. Tolman, *Acc. Chem. Res.*, 1997, **30**, 227.
12 R. Schenker, B. S. Mandimutsira, C. G. Riordan and T. C. Brunold, *J. Am. Chem. Soc.*, 2002, **124**, 13842.
13 B. S. Mandimutsira, J. L. Yamarik, T. C. Brunold, W. Gu, S. P. Cramer and C. G. Riordan, *J. Am. Chem. Soc.*, 2001, **123**, 9194.
14 S. Itoh, H. Bandoh, S. Nagatomo, T. Kitagawa and S. Fukuzumi, *J. Am. Chem. Soc.*, 1999, **121**, 8945.
15 S. Hikichi, M. Yoshizawa, Y. Sasakura, M. Akita and Y. Moro-oka, *J. Am. Chem. Soc.*, 1998, **120**, 10567.
16 S. Hikichi, M. Akita and Y. Moro-oka, *Coord. Chem. Rev.*, 2000, **198**, 61.
17 D. M. Roundhill, *Chem. Rev.*, 1992, **92**, 1.
18 X. Dai, P. Kapoor and T. H. Warren, *J. Am. Chem. Soc.*, 2004, **126**, 4798.
19 J. R. Khusnutdinova, P. Y. Zavalij and A. N. Vedernikov, *Organometallics*, 2007, **26**, 3466.
20 A. N. Vedernikov, S. A. Binfield, P. Y. Zavalij and J. R. Khusnutdinova, *J. Am. Chem. Soc.*, 2006, **128**, 82.
21 B. Longato, G. Bandoli and A. Dolmella, *Eur. J. Inorg. Chem.*, 2004, 1092.
22 K. Noro, Y. Ozawa, M. Taguchia and A. Yagasaki, *Chem. Commun.*, 2002, 1770.
23 E. Szuromi, S. Hui and P. R. Sharp, *J. Am. Chem. Soc.*, 2003, **124**, 10522.
24 E. Szuromi, J. Wu and P. R. Sharp, *J. Am. Chem. Soc.*, 2006, **128**, 12088.
25 M. A. Cinellu, G. Minghetti, F. Cocco, S. Stoccoro, A. Zucca and M. Manassero, *Angew. Chem., Int. Ed.*, 2005, **44**, 6892.
26 M. A. Cinellu, G. Minghetti, F. Cocco, S. Stoccoro, A. Zucca, M. Manassero and M. Arca, *Dalton Trans.*, 2006, 5703.
27 J. A. Keith, R. J. Nielsen, J. Oxgaard and W. A. Goddard, *J. Am. Chem. Soc.*, 2007, **129**, 12342.
28 S. Kannan, A. J. James and P. R. Sharp, *Polyhedron*, 2000, **19**, 155.
29 J. J. Li, W. Li and P. R. Sharp, *Inorg. Chem.*, 1996, **35**, 604.
30 A. Singh and P. R. Sharp, *Dalton Trans.*, 2005, 2080–2081.
31 T. M. Anderson, R. Cao, E. Slonkina, B. Hedman, K. O. Hodgson, K. I. Hardcastle, W. A. Neiwert, S. Wu, M. L. Kirk, S. Knottenbelt, E. C. Depperman, B. Keita, L. Nadjo, D. G. Musaev, K. Morokuma and C. L. Hill, *J. Am. Chem. Soc.*, 2005, **127**, 11948.
32 T. Hosokawa, M. Takano and S. I. Murahashi, *J. Am. Chem. Soc.*, 1996, **118**, 3990.
33 Y. Zhang, R. J. Puddephatt, L. Manojlovic-Muir and K. W. Muir, *Chem. Commun.*, 1996, 2599.
34 N. W. Aboelella, J. T. York, A. M. Reynolds, K. Fujita, C. R. Kinsinger, C. J. Cramer, C. G. Riordan and W. B. Tolman, *Chem. Commun.*, 2004, 1716.
35 U. Anandhi and P. R. Sharp, *Inorg. Chem.*, 2004, **43**, 6780.
36 I. Kaljurand, A. Kutt, L. Soovali, T. Rodima, V. Maemets, I. Leito and I. A. Koppel, *J. Org. Chem.*, 2005, **70**, 1019.
37 A. L. Llamas-Saiz, C. Foces-Foces and J. Elguero, *J. Mol. Struct.*, 1994, **328**, 297.
38 S. Wimmer, P. Castan, F. L. Wimmer and N. P. Johnson, *J. Chem. Soc., Dalton Trans.*, 1989, 403.
39 O. Crespo, A. Laguna, E. J. Fernandez, J. M. Lopez-de-Luzuriaga, P. G. Jones, M. Teichert, M. Monge, P. Pyykko, N. Runeberg, M. Schutz and H. J. Werner, *Inorg. Chem.*, 2000, **39**, 4786.
40 P. Pyykkö, *Chem. Rev.*, 1997, **97**, 597.
41 D. S. Gill and B. Rosenberg, *J. Am. Chem. Soc.*, 1982, **104**, 4598.
42 R. Faggiani, B. Lippert, C. J. L. Lock and B. Rosenberg, *Inorg. Chem.*, 1978, **17**, 1941.
43 R. Faggiani, B. Lippert, C. J. L. Lock and B. Rosenberg, *Inorg. Chem.*, 1977, **16**, 1192.
44 J.-P. Macquet, S. Cros and A. L. Beauchamp, *J. Inorg. Biochem.*, 1985, **25**, 197.
45 F. D. Rochon and R. Melanson, *Acta Crystallogr., Sect. C*, 1988, **44**, 474.
46 H. Shan and P. R. Sharp, *Angew. Chem., Int. Ed. Engl.*, 1996, **35**, 635.
47 H. Shan, A. J. James and P. R. Sharp, *Inorg. Chem.*, 1998, **37**, 5727.
48 A. Singh and P. R. Sharp, *Organometallics*, 2006, **25**, 678.
49 M. A. Jalil, T. Nagai, T. Murahashi and H. Kurosawa, *Organometallics*, 2002, **21**, 3317.
50 C. Tejel, M. A. Ciriano, M. Bordonaba, J. A. López, F. J. Lahoz and L. A. Oro, *Inorg. Chem.*, 2002, **41**, 2348.
51 L. Diez, P. Espinet and J. A. Miguel, *J. Chem. Soc., Dalton Trans.*, 2001, 1189.
52 J. J. Li, W. Li, A. J. James, T. Holbert, T. P. Sharp and P. R. Sharp, *Inorg. Chem.*, 1999, **38**, 1563.
53 F. A. Cotton and G. Wilkinson, *Advanced Inorganic Chemistry*, John Wiley and Sons, New York, 1988.
54 J. Vicente and A. Arcas, *Coord. Chem. Rev.*, 2005, **249**, 1135.
55 G. S. Hill, L. M. Rendina and R. J. Puddephatt, *J. Chem. Soc., Dalton Trans.*, 1996, 1809.
56 C. Diver and G. A. Lawrance, *J. Chem. Soc., Dalton Trans.*, 1988, 931.
57 M. Ferrer, A. Gutierrez, M. Mounir, O. Rossell, E. Ruiz, A. Rang and M. Engeser, *Inorg. Chem.*, 2007, **46**, 3395.
58 U. Fekl and R. van Eldik, *Eur. J. Inorg. Chem.*, 1998, 389.
59 E. Bielli, P. M. Gidney, R. D. Gillard and B. T. Heaton, *J. Chem. Soc., Dalton Trans.*, 1974, 2133.
60 G. Aúllon, G. Ujaque, A. Lledós, S. Alvarez and P. Alemany, *Inorg. Chem.*, 1998, **37**, 804.
61 U. Fekl, R. van Eldik, C. Richardson and W. T. Robinson, *Inorg. Chem.*, 2001, **40**, 3247.
62 F. H. Allen, *Acta Crystallogr., Sect. C: Cryst. Struct. Commun.*, 2002, **58**, 380.
63 P. A. Koz'min, V. V. Lapkin, L. K. Shubochkin, M. D. Surazhskaya, E. F. Shubochkina and T. B. Larina, *Zh. Neorg. Khim.*, 1988, **33**, 948.

64 P. Betz and A. Bino, *J. Am. Chem. Soc.*, 1988, **110**, 602.
65 I. J. B. Lin, J. S. Lai, L.-K. Liu and Y. S. Wen, *J. Organomet. Chem.*, 1990, **399**, 361.
66 V. V. Lapkin, M. D. Surazhskaya, T. B. Larina and P. A. Koz'min, *Zh. Neorg. Khim.*, 1993, **38**, 240.
67 V. V. Lapkin, M. D. Surazhskaya, L. K. Shubochkin, T. B. Larina and P. A. Koz'min, *Zh. Neorg. Khim.*, 1991, **36**, 609.
68 I. Ara, J. Fornies, L. Gabilondo and M. A. Uson, *Inorg. Chim. Acta*, 2003, **347**, 155.
69 J. J. Li and P. R. Sharp, *Inorg. Chem.*, 1994, **33**, 183.
70 W. Li, C. L. Barnes and P. R. Sharp, *J. Chem. Soc., Chem. Commun.*, 1990, 1634.
71 Y. Yang and P. R. Sharp, *Inorg. Chem.*, 1993, **32**, 1946.
72 J. Huheey, *Inorganic Chemistry: Principles of structure and reactivity*, Harper & Row, Philadelphia, PA, 1983.
73 E. Ilina and V. G. Kessler, *Polyhedron*, 2005, **24**, 3052.
74 L. K. Thompson, V. Niel, H. Grove, D. O. Miller, M. J. Newlands, P. H. Bird, W. A. Wickramasinghe and A. B. P. Lever, *Polyhedron*, 2004, **23**, 1175.
75 T. C. Higgs and C. J. Carrano, *Inorg. Chem.*, 1997, **36**, 298.
76 A. Yuchi, H. Murakami, M. Shiro, H. Wada and G. Nakagawa, *Bull. Chem. Soc. Jpn.*, 1992, **65**, 3362.
77 E. Carmona, J. M. Marin, M. Paneque and M. L. Poveda, *Organometallics*, 1987, **6**, 1757.
78 Y. B. Jiang, H. Z. Kou, R. J. Wang, A. L. Cui and J. Ribas, *Inorg. Chem.*, 2005, **44**, 709.
79 K. Shiren, S. Ogo, S. Fujinami, H. Hayashi, M. Suzuki, A. Uehara, Y. Watanabe and Y. Moro-oka, *J. Am. Chem. Soc.*, 2000, **122**, 254.
80 S. Hikichi, M. Yoshizawa, Y. Sasakura, H. Komatsuzaki, Y. Moro-Oka and M. Akita, *Chem.–Eur. J.*, 2001, **7**, 5011.
81 B. Bag, N. Mondal, S. Mitra and G. Rosair, *Chem. Commun.*, 2000, 1729.
82 M. Doering, G. Hahn, M. Stoll and A. C. Wolski, *Organometallics*, 1997, **16**, 1879.
83 A. B. Blake, E. Sinn, A. Yavari, K. S. Murray and B. Moubaraki, *J. Chem. Soc., Dalton Trans.*, 1998, 45.
84 B. C. Tzeng, S. C. Chan, M. C. W. Chan, C. M. Che, K. K. Cheung and S. M. Peng, *Inorg. Chem.*, 2001, **40**, 6699.
85 K. Matsumoto, N. Saiga, S. Tanaka and S. Ooi, *J. Chem. Soc., Dalton Trans.*, 1991, 1265.
86 R. Benn, B. Bogdanovic, P. Goettsch and M. Rubach, *Z. Naturforsch., B: Anorg. Chem. Org. Chem.*, 1983, **38**, 604.
87 J. Weiss, *Angew. Chem.*, 1982, **94**, 719.
88 B.-C. Tzeng, S.-C. Chan, M. C. W. Chan, C.-M. Che, K.-K. Cheung and S.-M. Peng, *Inorg. Chem.*, 2001, **40**, 6699.
89 A. N. Nesmeyanov, E. G. Perevalova, Y. T. Struchkov, M. Y. Antipin, K. I. Grandberg and V. P. Dyadchenko, *J. Organomet. Chem.*, 1980, **201**, 343.
90 D. Karshtedt, A. T. Bell and T. D. Tilley, *Organometallics*, 2004, **23**, 4169.
91 D. Karshtedt, A. T. Bell and T. D. Tilley, *J. Am. Chem. Soc.*, 2005, **127**, 12640.
92 R. van Asselt, C. J. Elsevier, C. Amatore and A. Jutand, *Organometallics*, 1997, **16**, 317.
93 A. Albinati, H. Lehner, L. M. Venanzi and M. Wolfer, *Inorg. Chem.*, 1987, **26**, 3933.